From Medical Biochemistry and Biophysics
Karolinska Institutet, Stockholm, Sweden

FIGHTING ISOASPARTATE

Jijing Wang

Karolinska Institutet

Stockholm 2022

Published by Karolinska Institutet.

Printed by Universitetsservice US-AB, 2022

ISBN 978-91-8016-761-1

Cover illustration: Isoaspartate as a molecular clock for aging and neurodegeneration.
Designed by Ziqing Chen and Jijing Wang.

FIGHTING ISOASPARTATE

THESIS FOR DOCTORAL DEGREE (Ph.D.)

By

Jijing Wang

The thesis will be defended in public at Samuelsson-Salen, Floor 1, Tomtebodavägen 6, Solna, 23rd Sept, 2022 at 9.30 AM

Principal Supervisor:

Prof. Roman A. Zubarev

Karolinska Institutet

Department of Medical Biochemistry and Biophysics

Division of Physiological Chemistry I

Co-supervisor(s):

Dr. Sergey Rodin

Uppsala University

Department of Surgical Sciences

Opponent:

Prof. Stefan Teipel

German Center for Neurodegenerative Diseases (DZNE)

Department of Clinical research Rostock/Greifswald

Examination Board:

Dr. Lars Tjernberg

Karolinska Institutet

Department of Neurobiology, Care Sciences and Society

Division of Neurogeriatrics

Prof. Eric Westman

Karolinska Institutet

Department of Neurobiology, Care Sciences and Society

Division of Clinical Geriatrics

Dr. Muriel Priault

French National Centre for Scientific Research

Institute for Cellular Biochemistry and Genetics (IBGC)

To my family

献给我的家人

“Rome was not built in one day.”

“不积跬步，无以至千里。” —— 荀子《劝学》

ABSTRACT

Isoaspartate (IsoAsp) is a damaging amino acid residue generated either from asparagine (Asn) deamidation or aspartate (Asp) isomerization. Both reactions are spontaneous in physiological conditions and require no enzymes. In isoAsp, a CH_2 group is rearranged from the side chain and extends the polypeptide backbone. The accumulation of isoAsp disrupts protein structures and functions, making them prone to aggregation, and eventually contributes to the onset of Alzheimer's disease (AD) and other neurodegenerative diseases (NDDs). Since the mass of isoAsp is the same as Asp, and only +0.98 Da different than Asn, the quantification of isoAsp requires high sensitivity and specificity of the analysis. Moreover, it is very difficult to develop a monoclonal antibody against isoAsp with high specificity. Although Asn deamidation is considered irreversible, there is an enzyme protein $_L$-isoaspartyl methyltransferase (PIMT) that mitigates its damaging effect. PIMT methylates isoAsp using S-adenosylmethionine (SAM) as a methyl donor. Upon methanol loss, methylated isoAsp spontaneously becomes normal $_L$-Asp in a minority (< 25%) of cases or more probably isoAsp again (≥ 75%). However, with age SAM production declines, rendering repair insufficient. This may result in isoAsp accumulation in long-lived proteins, including human serum albumin (HSA), the most abundant protein in blood. In the present thesis, we depict different ways to "fight" isoAsp, either via its early detection or exploring the repair mechanism, which we believe render avenues to fighting aging and age-related diseases.

In **Paper I**, we developed a monoclonal antibody (mAb) specific to isoAsp in an important domain of HSA, and characterized it via DNA/amino acid sequencing, kinetic analysis, paratope mapping, glycosylation analysis, etc. We also quantified the isoAsp level in HSA of the blood of 100 healthy donors, the histogram of which resembled the normal distribution. In **Paper II**, for the first time we demonstrated that isoAsp-containing HSA forms aggregates with reduced binding capacity toward amyloid beta (Aß) peptide and phosphorylated tau (p-Tau) protein. Using the mAb raised in **Paper I** and size exclusion chromatography, we found a significant increase of isoAsp level in HSA and its aggregates of the patients with AD compared with controls. We also discovered in AD group a significantly decrease of antibodies against isoAsp in HSA, as well as an increase of free Aß not bound with HSA. Based on the findings, we updated the isoAsp hypothesis of AD, supporting the role of isoAsp accumulation as a triggering factor in AD. In **Paper III**, we validated the results in **Paper II**, and further explored the capacity of isoAsp in diagnostics of other NDDs. The most significant finding was the best performance of isoAsp-related biomarkers in mild cognitive impairment (MCI) detection compared with other blood biomarkers. In addition, the levels of isoAsp in HSA and its antibodies significantly correlated with cognitive decline. In **Paper IV**, we discussed theoretical considerations supporting the possibility of a full repair of isoAsp to Asn and reported the first experimental evidence on the reversibility of isoAsp formation via protein succinimide/isoaspartate ammonia ligase (PSIAL) activity. We also discovered PSIAL activity in the recombinant cytoplasmic human aspartate aminotransferase (GOT1).

LIST OF SCIENTIFIC PUBLICATIONS

I. **Wang J**, Lundström SL, Seelow S, Rodin S, Meng Z, Astorga-Wells J, Jia Q, Zubarev RA. First immunoassay for measuring isoaspartate in human serum albumin. *Molecules*. 2021; 26(21):6709. https://doi.org/10.3390/molecules26216709.

II. **Wang J**, Guo C, Meng Z, Zwan MD, Chen X, Seelow S, Lundström SL, Rodin S, Teunissen CE*, Zubarev RA*. Testing the link between isoaspartate and Alzheimer's disease etiology. *Alzheimer's and Dementia*. 2022;1-12. https://doi.org/10.1002/alz.12735.

III. **Wang J***, Zhang Y*, Shen X, Han J, Cui M, Tan L, Dong Q, Zubarev RA*, Yu J*. Isoaspartate-related blood biomarkers show promise for early diagnostics of neurodegeneration. *Manuscript*.

IV. **Wang J**, Rodin S, Dibavar AS, Zhang X, Zubarev RA. First experimental evidence for reversibility of ammonia loss from asparagine. *International Journal of Molecular Sciences*. 2022; 23(15):8371. https://doi.org/10.3390/ijms23158371.

*: These authors contributed equally.

CONTENTS

LIST OF ABBREVIATIONS

AD	Alzheimer's disease
Asn	asparagine residue
Asp	aspartate residue
Aβ	amyloid beta
BBB	blood-brain barrier
CBD	corticobasal degeneration
CID	collision-induced dissociation
CSF	cerebrospinal fluid
DLB	dementia with Lewy bodies
ECD	electron capture dissociation
ECL	electrochemiluminescence
ELISA	enzyme-linked immunosorbent assay
ETD	electron transfer dissociation
FTD	frontotemporal dementia
GFAP	glial fibrillary acidic protein
Gln	glutamine
GOT1	cytoplasmic aspartate aminotransferase
HCD	higher-energy collisional dissociation
HSA	human serum albumin
LC-MS/MS	liquid chromatography and tandem mass spectrometry
isoAsp	isoaspartate
mAbs	monoclonal antibodies
MCI	mild cognitive decline
MoCA	Montreal Cognitive Assessment
MMSE	Mini-Mental State Examination
NDDs	neurodegenerative diseases
NfL	neurofilament light chain
NIA-AA	National Institute on Aging-Alzheimer’s Association
PET	positron emission tomography
PD	Parkinson’s disease
PIMT	protein $_{L}$-isoaspartyl methyltransferase
PSIAL	protein succinimide/isoasapartate ammonia ligase
PSP	progressive supranuclear palsy
SAM	*S*-adenosylmethionine
SAH	*S*-adenosylhomocysteine
p-Tau	phosphorylated tau
RT	retention time
t-Tau	total tau
VaD	vascular dementia

1 INTRODUCTION

1.1 ALZHEIMER'S DISEASE (AD) AND OTHER NEURODEGENERATIVE DISEASES (NDDS)

1.1.1 Overview

Alzheimer's disease (AD) is the most common neurodegenerative disorder causing senile dementia. It was reported by World Health Organization in 2021 that around 55 million people have dementia worldwide, and that AD contributes to 60-70% of the cases [1]. More specifically, it was evaluated that one in ten people over the age of 65 and more than 30% of people over 85 have AD [1, 2]. There are about 10 million new cases every year, and the world's population of dementia is expected to reach 139 million by 2050 [1].

The disease pathology usually initiates decades before the onset of the symptoms, which can be typically identified on the histopathological level, as the deposition of extracellular senile plaques formed by amyloid-beta (Aβ) protein and neurofibrillary tangles (NFTs) composed of hyper-phosphorylated Tau (p-Tau). Such kind of accumulation can also be discovered in non-demented people suffering from mild cognitive impairment (MCI) [3]. Currently no cure for AD exists and its diagnosis can be complicated. Besides AD, NDDs also include vascular dementia (VaD), dementia with Lewy bodies (DLB), frontotemporal dementia (FTD), Parkinson's disease (PD), progressive supranuclear palsy (PSP), corticobasal degeneration (CBD), etc. Different pathological events are involved in NDDs, including Aβ pathology, tau pathology, neuronal injury, inflammation and vascular dysregulation (**Figure 1**).

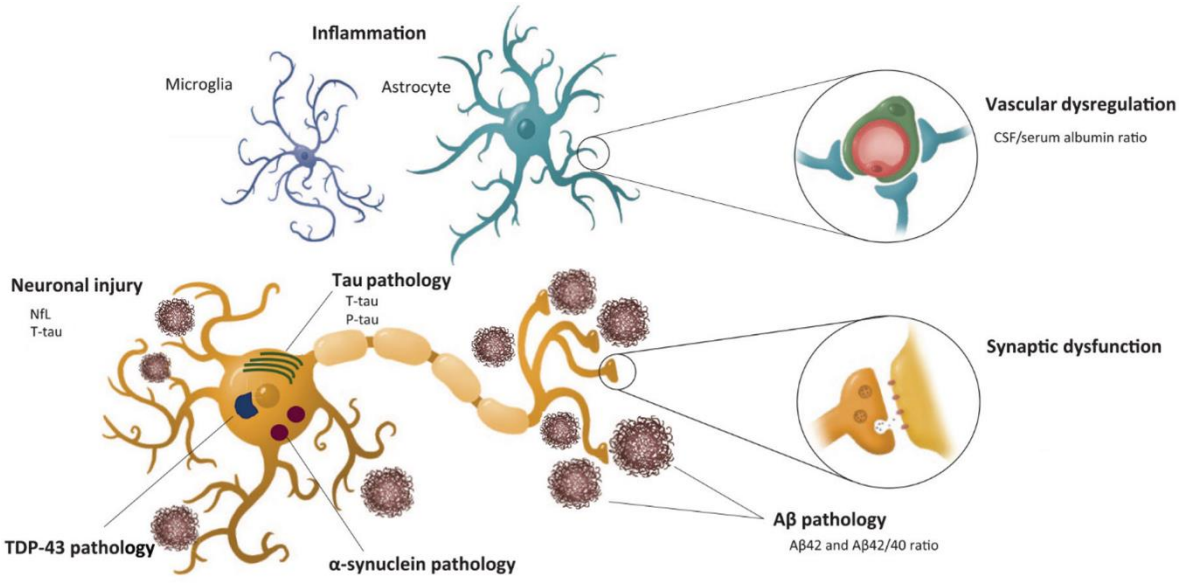

Figure 1. Pathological events in NDDs and their corresponding fluid biomarkers. Adapted from Mila-Aloma, M., et al. Therapeutic Advances in Neurological Disorders, 2019 [4]. Abbreviation: Aβ, β-amyloid; TDP-43, transactive response DNA-binding protein 43; t-tau, total tau.

1.1.2 Diagnostic biomarkers

The clinical diagnoses of AD have until recently been based on memory deficiency evaluation of recalls, positron emission tomography (PET) imaging of amyloid deposits, and cerebrospinal fluid (CSF) testing for p-Tau protein and Aβ peptide [5, 6]. Similar methods have also been used in other NDDs based on different biomarkers (Table 1). The definite AD diagnosis is still done by postmortem brain autopsy, while the diagnoses given during the lifetime of the patient are "probable AD" and "possible AD" [7]. A study in 2012 uncovered that such diagnostics misses 13-29% of AD cases, while 29-59% of presumed AD cases do not find postmortem confirmation [8]. The accuracy of diagnoses for other NDDs (e.g., VaD, FTD, DLB, PSP) could be even lower [9-12], thus easily accessible and accurate clinical diagnostic biomarkers are highly needed, especially during the early disease stages.

The National Institute on Aging and Alzheimer's Association updated the diagnostic recommendations for different stages of AD in 2018. Within the "Research Framework", AD diagnosis is not based on the clinical symptoms/signs or postmortem examination, but on biomarkers in living individuals. The known biomarkers are grouped into deposition of Aβ, p-Tau, and neurodegeneration [AT(N)]. This ATN classification system is flexible in that new biomarkers can be added when they become available. It is even allowed that Aβ plaques and neurofibrillary p-Tau tangles may not be the ultimate cause of AD pathogenesis [13]. However, observationally Aβ plaques with or without neurofibrillary p-Tau remain the molecular features most strongly linked to AD [14-16], and thus any AD etiology hypothesis should try to explain Aß aggregation in the brain.

During the last decade, blood-based biomarkers have been extensively studied and some have been used for preclinical diagnosis of AD with the advantage of non-invasiveness (**Figure 2**, **Table 1**). Most of these biomarkers focus on Aβ (Aβ42, Aβ40, Aβ42/Aβ40) and Tau (total-Tau, p-Tau181, p-Tau217, p-Tau231), re [17-21]. Some others have emerged recently as well, like neurofilament light chain (NfL) and glial fibrillary acidic protein (GFAP) [22-25]. Compared with individual levels of plasma Aβ42 and Aβ40, the ratio Aβ42/Aβ40 tends to better reflect the brain Aβ pathology and has been regarded as a promising blood biomarker for AD [26]. While blood total-Tau has been used more in detecting the acute injury of neurons, the performance of the plasma p-Tau biomarker depends upon the phosphorylation position(s). In recent reports, the plasma p-Tau181, p-Tau217 and p-Tau231 have shown strong association with amyloid and tau PET results [27, 28], as well as the capability of distinguishing AD from other dementia types. Thus p-Tau has been recognized as a robust blood biomarker for AD pathology [12]. Besides p-Tau, plasma NfL and GFAP have been confirmed to significantly increase in various types of NDDs [9-12]. The quantification methods of blood biomarkers have in recent years focused more on the simplicity and speed of analysis, such as in enzyme-linked immunosorbent assay (ELISA) [29-31], single molecule array (Simoa) [32-34], and electrochemiluminescence (ECL) [35, 36]. To date, plasma NfL assay is already available in clinical laboratory practice for NDD diagnoses in Sweden, the Netherlands and France [37], while plasma GFAP was authorized by FDA for diagnostics of mild traumatic brain injury (TBI) [38]. The Alzheimer's Association has also just announced the recommendations of starting using blood biomarkers cautiously in clinical practice [39].

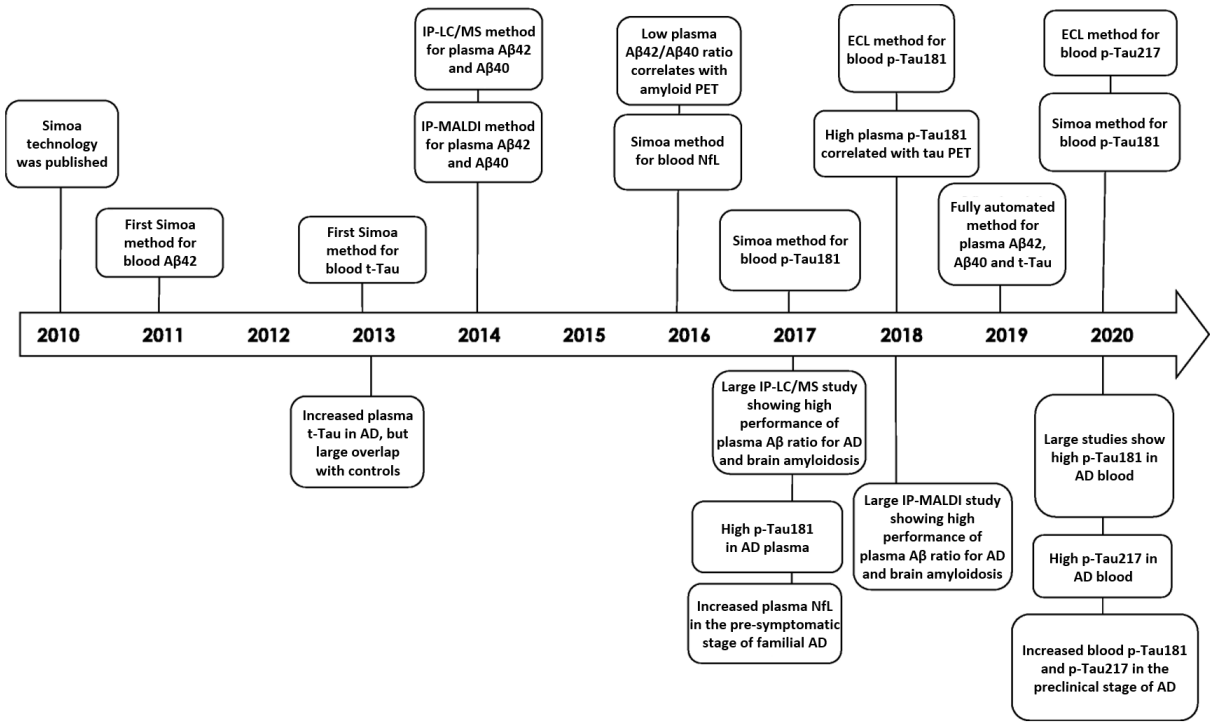

Figure 2. Timeline for blood biomarker developments during the last decade. Abbreviations: IP-LC/MS, immunoprecipitation liquid chromatography-mass spectrometry; IP-MALDI, immunoprecipitation matrix-assisted laser desorption/ionization. Zetterberg, H., Blennow, K. Mol Neurodegener, 2021 [37].

Table 1. Blood-based biomarkers for neurodegeneration

Biomarker	Pathological events	Disease of interest	Methods
Aβ42; Aβ42/Aβ40	Amyloidosis	AD, FTD, PD	ECL, IP-MS, Simoa
t-Tau	Axonal loss, neuronal injury	AD, FTD	Simoa
p-Tau181, p-Tau217	Tau pathology	AD	ECL, Simoa
NfL	Axonal loss	AD, FTD, PD, MS, ALS	ECL, Simoa, ELISA
GFAP	Astrogliosis, astrocytic activation	AD, FTD, MS	ECL, ELISA

1.2 ISOASPARTATE (ISOASP)

1.2.1 Deamidation and isoAsp

Deamidation is a loss of ammonia, and it is one of the most abundant posttranslational modifications (PTMs) in proteins. It is a spontaneous chemical reaction proceeding without an enzyme even at physiological conditions [40]. As soon as the protein molecule is expressed, deamidation starts, acting both *in vivo* and *in vitro*, and the reaction can be accelerated in alkaline conditions or at high temperature (> 37 ˚C) [41]. Deamidation occurs from asparagine (Asn, N) or, less frequently, from glutamine (Gln, Q) residues. Deamidation of Asn as well as isomerization of aspartate (Asp, D) residues result in the unstable cyclic succinimide (Succ), which in around 75% of the cases hydrolyzes by attaching a water molecule to become a ß-isomer of Asp – isoaspartate (IsoAsp) [40, 42]. In other cases, this intermediate converts to L-Asp. Asn deamidation rates depend upon the sequence context and protein 3D structure [43, 44], with the highest rates occurring in the Asn-Gly and Asn-Ser sequence motifs [45].

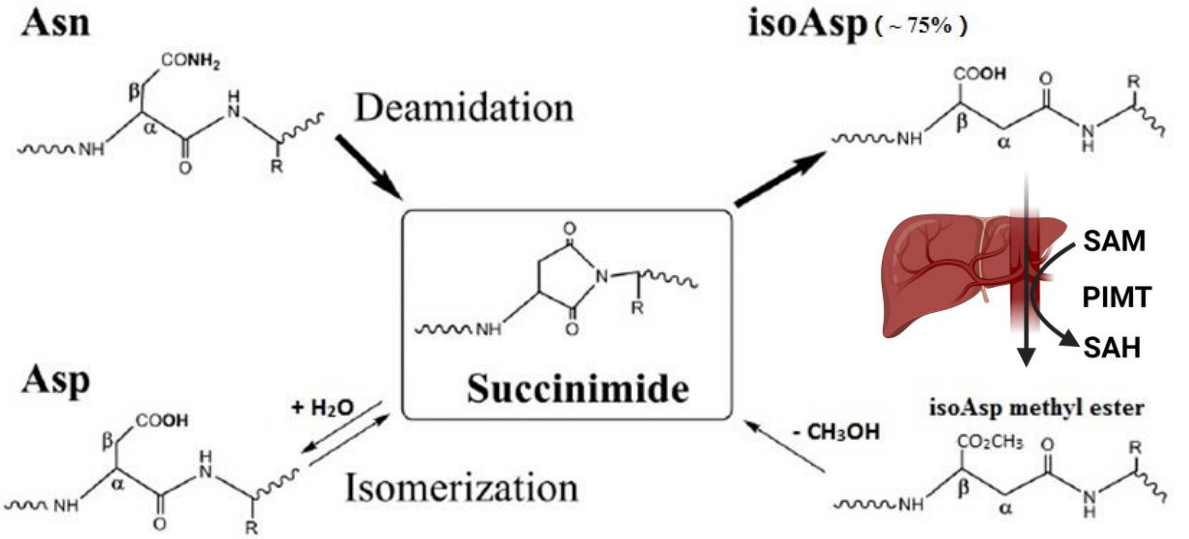

Figure 3. Isoaspartate (IsoAsp) formation. Abbreviations: SAM, *S*-adenosylmethionine; PIMT, protein L-isoaspartyl methyltransferase; SAH, *S*-adenosylhomocysteine.

IsoAsp is a damaging amino acid. In isoAsp the polypeptide backbone is extended by a CH_2 group that rearranges from the side chain and inserts itself between the α-carbon and carbonyl (**Figure 3**). Such insertion disrupts the protein structures (α-helices and ß-sheets), as well as protein functions. For example, the deamidated epidermal growth factor (EGF) in human no longer binds to the corresponding receptor, and therefore stops acting as a growth factor [46]. Moreover, isoaspartyl peptides are difficult to proteolytically degrade in antigen-presenting cells, rendering such peptides immunogenic, and thus initiating systemic autoimmune diseases, such as systemic lupus erythematosus, multiple sclerosis, etc. [47-49]. Furthermore, it was hypothesized that deamidation might alter the islet microenvironment during the beginning phase of the type 1 diabetes, making non- ß cell-specific proteins become antigenic and specific to ß cells [50, 51]. IsoAsp can also play a regulatory role - it promotes apoptosis induced by DNA damage [52] and suppresses p53 activity [53].

1.2.2 Repair of isoAsp

The defense mechanisms against isoAsp build-up can theoretically include proteases, repair, and antibodies. Deamidation of asparaginyl is considered irreversible, and no pathway from isoAsp back to L-Asn has been found or proposed theoretically. In addition, isoaspartyl bonds are resistant to most proteolytic enzymes [54, 55] and can be cleaved only after the protein is degraded to a dipeptide by a few isoaspartyl dipeptidases known through *in vitro* studies [56-58]. For instance, recombinant human glycosylasparaginase produced in mouse cells catalyzes the hydrolysis of isoaspartyl peptides *in vitro*, and it is believed to play an important role in the metabolism of isoaspartyl peptides [57]. Human ASRGL1 protein recombinantly produced in bacteria has been shown to exhibit the β-aspartyl peptidase activity to cut different isoaspartyl dipeptides *in vitro* [56]. However, it is still unclear exactly how human cells process isoaspartyl dipeptides *in vivo*.

Nevertheless, there is an enzyme named protein L-isoaspartyl methyltransferase (PIMT) that repairs L-Asp isomerization and mitigates the damaging effect of Asn deamidation. PIMT methylates isoAsp using *S*-adenosylmethionine (SAM) as a methyl donor that becomes *S*-adenosylhomocysteine (SAH), while methylated isoAsp loses methanol molecule spontaneously to become either L-Asp in no more than 25% of the cases or more likely (≥ 75%) isoAsp again [40, 42] (**Figure 3**). This low-efficiency process converts isoAsp to L-Asp instead of the original L-Asn, and it takes on average four cycles of methylation to repair > 80% of a single residue. Worse yet, the biochemical properties of Asp are quite different from those of Asn, including a different pI and pKa. Therefore, PIMT-mediated repair is in fact a "quick fix" rather than true repair.

A proteomics study of the brain tissue has confirmed that the isoAsp level was significantly increased in PIMT-knockout mice compared to wild type mice [59]. Depleting PIMT gene elicited isoAsp accumulation in all tissues measured, especially in the brain [60, 61]. PIMT regulates p53 activity [53], while PIMT suppression induces activation of P13K/Akt and insulin signaling [62, 63] as well as hyperactivation of EGF-stimulated MEK-ERK pathway [64].

The quick fix of isoAsp by PIMT and SAM occurs mostly in liver, where the blood flow passes 20–25 times per day. The majority of SAM molecules are synthesized in liver and so is the human serum albumin (HSA), the most abundant protein in blood. On average, HSA circulates in blood for around 25 days [65], thus passing by the liver approximately 500–600 times before removal. On each passage, the isoAsp residues are converted to L-Asp by PIMT and SAM, significantly restoring the protein structure and solubility. Nevertheless, the production of SAM declines as a person ages [66], rendering PIMT-mediated repair insufficient, which may lead to the accumulation of isoAsp in long-lived proteins, including HSA [67].

1.2.3 Quantification of isoAsp in proteins

The mass of isoAsp is exactly the same as aspartate, and differs only by +0.98 Da to Asn. Thus, the measurement of isoAsp requires high sensitivity and specificity, especially in complex protein mixtures like biofluid samples. For the past decade, the isoAsp quantification has been performed by liquid chromatography coupled to tandem mass spectrometry (LC-MS/MS) [20].

The fragmentation technique electron capture/transfer dissociation (ECD or ETD) provides an isoAsp-specific fragment [68], which ensured the required sensitivity and specificity of isoAsp detection. However, there are several obvious drawbacks of this method. One drawback is the demand for overnight tryptic digestion of proteins before the LC-MS/MS analysis, which can cause artificial deamidation masking the biological differences [45, 46]. The other disadvantages are the low throughput, time consuming routines, high analysis cost and necessity of specialized technicians. Apart from LC-MS/MS, a kit called ISOQUANT was developed by Promega more than 20 years ago [69]. The target protein or protein mixture sample was incubated together with enzyme PIMT and cofactor SAM. The methylation product of the PIMT repair, SAH, was then detected by reversed phase high-performance liquid chromatography (HPLC). The isoAsp occupancy was calculated by comparing the chromatographic peak area with a standard curve. This method, though having lower requirement for instrumentation, still exhibited similar weakness as LC-MS/MS, and thus are not widely used. Hence, better ways to quantify isoAsp than the two methods above are needed. In fact, ELISA avoids the drawbacks described above as it requires no protein digestion with the advantages of low cost, high throughput and being scalable, provided a monoclonal antibody highly specific to isoAsp is obtained (which has long been the main obstacle).

1.2.4 IsoAsp and NDDs

The consequences of isoAsp formation and accumulation are severe not only for the affected proteins, resulting in loss of their function, but also for the whole organism. Deamidation sets in motion a protein aggregation cascade that can ultimately lead to deteriorated health and ageing. It has been hypothesized that deamidation may also cause neurodegeneration, and result in AD [70, 71]. The hypothetical link between isoAsp and NDDs can be traced back to the early 1990s, when the protein aging hypothesis was first proposed [72]. The hypothesis suggested that isoAsp accumulation initiates the cascade of effects ultimately leading to AD. Several subsequent studies strengthened the link between the isoAsp formation and Aβ aggregation. For instance, it has been shown that isoAsp is present not only in extracellular deposits of AD brain, but also in amyloid-bearing blood vessels [70]. An immunostaining study in core plaques demonstrated that the isoAsp modified Aβ were more significantly present in brains of patients with AD [73]. It has been shown that the conformation, aggregation and toxicity of Aβ could be highly influenced by the formation of isoAsp [74, 75]. One older hypothesis directly suggested that isoAsp formation in the Aß peptides, particularly Asp isomerization in position 7 (isoAsp7-Aß), leads to Aß aggregation and ultimately to AD (**Figure 4**) [76]. This theory has been supported over the years by several studies [77-79].

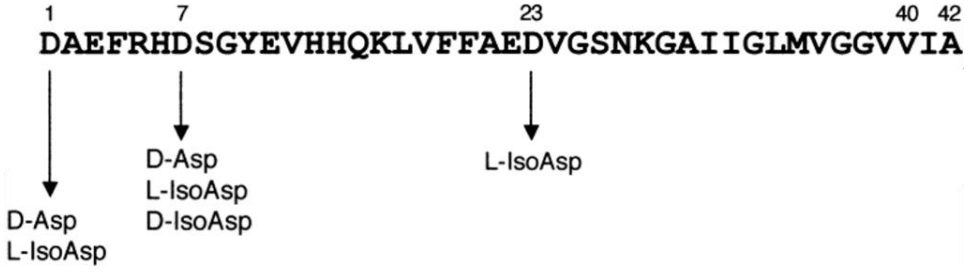

Figure 4. Isomerization and racemization at the Asp residue of Aß found in AD brains. All Asp residues at positions 1, 7, and 23 in Ab were isomerized or racemized. Adapted from Shimizu et al., Biol Pharm Bull, 2005 [80].

Aß peptides are usually produced by astrocytes and neurons in the brain, and secreted into the extracellular fluid, where they face two basic fates. One is the clearance by enzymatic degradation or receptor-mediated export to blood or CSF. However, how the Aβ clearance from the brain to the venous blood is still obscure [81], but it appears that on the other side of the blood-brain barrier (BBB), HSA picks up Aß possibly via intermediates, and transports it to the liver and kidneys, where Aß is metabolized [82-84]. The alternative fate is the aggregation into neurotoxic oligomers and longer polymers that can ultimately be deposited as amyloid plaques. Any bottleneck in Aß clearance can lead to an elevated Aß level in the brain, prolong its residence time there, and thus increase the extent of Asp-7 isomerization. As the latter process contributes to facile Aß aggregation, a bottleneck in Aß clearance elevates the AD risk.

Application of mass spectrometry to blood samples has confirmed that the elevated isoAsp levels in blood are closely associated with AD [85]. A proteomic research study also confirmed that the easily aggregated proteins, such as fibrin and fibrinogen, are strongly associated with rapid AD development [86]. These proteins tend to interact with Aβ, resulting in Aβ fibrillization and formation of fibrin clots resistant to degradation in the brain [86, 87]. The protease inhibitors also correlate with AD, while the proteins delaying the AD development are those participating in clearing protein aggregates, like proteases and immune-response proteins [86]. Both studies were carried out by LC-MS/MS, which is a sensitive but also expensive method for isoAsp analysis. The isoAsp content in abundant blood proteins and the levels of these proteins could differentiate AD and healthy controls with around 80% accuracy [85].

1.3 HUMAN SERUM ALBUMIN (HSA) AND NDDS

Being the most abundant protein in blood, HSA represents more than half of the protein content in blood. It is synthesized in liver, and also appears in lymph, saliva, cerebrospinal and interstitial fluid [88]. HSA is an important protein responsible for many physiological functions, such as regulating plasma colloid osmotic pressure [89] and inhibiting lipid peroxidation in plasma [90]. More importantly, it serves as a main carrier for transporting a variety of endogenous and exogenous compounds, including metals [91], fatty acid [92], hemin [93], thyroxin [94] and drugs [95]. Also, HSA binds and carries 90% of the Aβ in blood plasma [96]. Furthermore, as one of the most potent Aβ sequestering agents, HSA plays a special role in AD etiology. Model organism studies indicated that serum albumin inhibits Aβ aggregation [97] and fibrillation [98-100] by binding Aβ monomers or oligomers, while a Japanese cohort demonstrated the decreased serum levels of albumin-Aβ complexes in AD, which was also associated with increased CSF p-Tau levels [101]. Other human studies have revealed the association of low HSA levels with cognitive impairment [102, 103] as well as AD [104, 105], multiple sclerosis (MS) and amyotrophic lateral sclerosis (ALS) [106-108]. A recent study (n = 396) has proved that the HSA level as a continuous variable has a negative association with Aβ deposition in older adults [109]. This result was compatible with the earlier finding that HSA can regulate the fiber growth of Aß in the brain interstitium [99].

The protease clearance path of brain Aß can be hampered by isoaspartyl bond formation in deamidated or isomerized Aß residues, which occur more likely if the residence time of Aß prolongs or the isoAsp repair becomes inefficient. The latter can happen if the brain SAM level drops, as is the case in AD [110-112]. Interestingly, the clearance pathway via receptor-mediated export to blood plasma, can be hampered by a reduced plasma ability to uptake or remove Aß. The uptake reduction happens when HSA concentration decreases, or the ability of an average HSA molecule to carry Aß peptides diminishes.

Notably, HSA has a series of metal-binding sites that are mainly responsible for metal binding in blood [113]. According to the metal hypothesis of AD, metals such as copper and iron are able to form complexes with Aβ and are also found at particularly high levels in amyloid plaques [114, 115]. It has been revealed that HSA can reduce the interaction between Aβ and aberrant Cu (II), and revert copper-induced Aβ aggregation, thus rescuing cells from its toxicity [116]. Besides, dysregulated copper ions may induce and exacerbate tau hyperphosphorylation and fibrillization, eventually resulting in the neuronal death, synaptic failures, and cognitive decline which are observed in AD [117]. It is plausible that HSA molecules with abnormally increased isoAsp levels might not be able to interrupt the binding of metals with Aβ or p-Tau, but this has not been reported in literature yet.

Apart from being a main transporter in blood, albumin is also the most abundant protein in CSF, and the CSF/serum albumin ratio has been widely used in clinical practice to measure BBB function [4, 118]. This ratio was found to be increased in various dementia types, and it was associated with CSF levels of NfL but not with other CSF biomarkers for AD, indicating that BBB damage is a common phenomenon of cerebrovascular pathology [119].

1.4 ANTIBODIES

1.4.1 Structures and types of antibodies

Antibodies, also known as immunoglobulins (Ig), are large proteins produced by the humoral immune system to neutralize pathogens, such as pathogenic bacteria and viruses. The Ig structure was first proposed by Paul Ehrlich, which led to a series of subsequent studies on its structures and function studies [120]. The heavy and light chains are connected by disulfide bonds, forming two antigen-binding fragments (Fab) of the Y-shaped structure. The stem part-crystallisable fragment (Fc) determines the isotype of an antibody. Each heavy chain or light chain contains one variable (V) domain (**Figure 5**). The antigen epitope is recognized by the antibody paratope via complementarity-determining regions (CDRs) in variable domains, which are hypervariable. The five main isotypes of antibodies in human (IgG, IgA, IgE, IgM and IgD) differ in structure, biological activity and relative abundance in plasma. Among them, IgG is the most abundant one with four subclasses (IgG1, IgG2, IgG3 and IgG4).

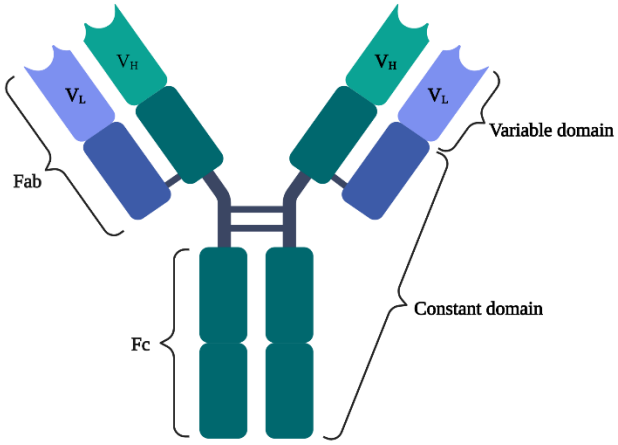

Figure 5. The structure of immunoglobulin. The fragment antigen-binding (Fab) regions form two arms of the Y shape. The variable domain in the heavy chain (V_H) and light chain (V_L) contains three hypervariable complementarity-determining regions (CDRs) that define antibody binding to the antigen.

1.4.2 Monoclonal antibodies (mAbs)

Monoclonal antibodies (mAbs) are often produced by the hybridoma technology that was first introduced by Köhler and Milstein in 1975 [121]. This technology enables the production of unlimited amounts of mAbs that are specific to an epitope of certain antigens. In short, a host animal is immunized with the antigen (usually, a peptide conjugated with a carrier protein) to induce an immune response and initiate the maturation of B cells. Then the B cells are isolated from the spleen of the host animal and fused with myeloma cells to generate hybridomas. After several rounds of screening and selection, the clones that produce the best mAbs are selected for subsequent purification [122, 123]. Being specific to one epitope, the mAbs are sensitive to the conformational changes of the antigen. In contrast, polyclonal antibodies can be specific to multiple epitopes of the same antigen, and the conformational changes in the latter do not influence the binding very much [124]. So far, more than 600 therapeutic mAbs have been used in clinical trials over the world [125-127]. Of these, more than 104 therapeutic mAbs have been approved by the European Union (EU) or United States (US) and are currently on the market [128]. Many of them were designed to treat human diseases such as cancers, neurological disorders, immunological and metabolic diseases [129]. More therapeutic mAbs have emerged since the pandemic of coronavirus disease (COVID-19), and the technology and strategies have been refined to enable rapid clinical evaluation [127, 130].

1.4.3 Characterization of antibodies

Antibodies are usually characterized by their sequences, PTMs (e.g., glycosylation), and the parameters of binding to their antigens.

The genes of variable regions in antibodies have been available by sequencing since late 1980s [131], when the technology of polymerase chain reaction (PCR) and Sanger sequencing became widely used. Normally, total RNA (or messenger RNA) is extracted from B cells in blood or bone marrow, or from hybridoma cells. Then by reverse-transcription with an oligo primer, cDNA is created. Both the V_H and V_L domains are then amplified by PCR using

variable domain primers. Since large-scale sequencing for high throughput became available, multiplex oligonucleotide primers have been designed to amplify nearly all antibody variable genes [132]. This has particularly boosted the progress of developing phage display libraries for novel antibody discoveries, which won the 2018 Nobel Prize in Chemistry [133]. The next generation sequencing has recently been combined with phage display for deeper sequencing and more diverse positive clones [134, 135].

Nevertheless, the complexity of a full antibody repertoire from B cells remains a challenge for DNA/RNA sequencing. This challenge can only be addressed by single-cell techniques that however introduce cloning biases, let alone clone amplification biases from PCR [136]. In contrast, de novo sequencing of amino acids by MS/MS achieves sequencing antibodies purified directly from blood plasma without the necessity to isolate and sequence any B cells [137, 138]. Digestions by different enzymes coupled with complementary fragmentation techniques, collision-induced dissociation (CID), HCD or ETD, have enabled full-length de novo sequencing of antibodies from plasma [138, 139]. Moreover, one can synthesize the antibody with the deduced sequence and validate its specificity by showing that the synthetic antibody binds more to the test antigen than to the decoy antigen.

However, identification of PTMs in antibodies still remains challenging. PTMs can occur in any stage of antibody production and secretion. All antibodies possess glycosylation, and each isotype has a unique N-linked carbohydrate attached to a conserved Asn residue in the constant domain of heavy chains, which results in different conformations and functions of antibodies [140, 141]. Different from N-linked glycosylation with complete transfer of monosaccharide chain, O-linked glycosylation is more like a sequential attachment of single monosaccharide units. Both glycans can be found in the variable domains, influencing the specificity of antibodies [142]. So far, most studies to identify PTMs of antibodies have relied on MS/MS.

1.4.4 Antibodies and isoAsp

If isoaspartyl moieties are not repaired or quickly removed, the isoaspartyl-containing self-polypeptide can become immunogenic. For instance, PIMT knockout mice that cannot repair isoAsp and accumulate isoAsp in many organs, develop a hyperproliferative T cell response and a systemic autoimmune pathology [62]. Thus, antibodies can be raised in animals against isoAsp-containing epitopes in otherwise native proteins. Due to the small size of the isoAsp residue, it is difficult to create a pan-isoAsp antibody that would be specific to isoaspartyl regardless the sequence context. To this date, there was no report in literature on native human antibodies against deamidated human proteins; nevertheless, some polyclonal antibodies [70, 143, 144] and a set of monoclonal antibody [145] specific to isoAsp have been reported, but still have not been commercialized. One monoclonal anti-isoAsp antibody was used to demonstrate the presence of isoAsp7 in extracellular Aβ deposits in mouse AD brain as well as amyloid-bearing vessels, supporting previous observations via using polyclonal isoAsp7-Aβ antisera [45, 98]. The treatment of anti-isoAsp7-Aβ antibodies on 5×FAD mice showed reduced abundance of total Aβ in brain, inducing attenuation of amyloid pathology and amelioration of cognitive impairment, suggesting the treatment efficacy of such antibodies in an animal model.

1.4.5 Antibodies and AD

So far, one of the most extensively pursued strategies in AD therapies has been the passive immunotherapy, through administration of exogenous mAbs. Targeting the main hallmarks of AD, researchers have developed quite a few antibodies against Aβ, its oligomers and aggregates for clinical trials. However, until now all tested anti-Aß therapies have failed to demonstrate consistent therapeutic capacity of slowing disease progress, including recent (after 2019) ones [126, 127]. Among those that have been tested in clinical trials, only the mAb BAN2401 and Aducanumab have shown positive trends [127-129]. The US Food and Drug Administration (FDA) just approved Aducanumab as the first therapy for AD treatment via an Accelerated Approval on June 7, 2021, as it reduced the level of amyloid plaques in AD brains both dose- and time-dependently [130]. This has been marked as a milestone in the history of AD treatment; however, the clinical benefits could only be verified after the post-approval studies. Adding to the setbacks from previous trials targeting Aß, the first mAb against Tau has just failed, calling for more studies on causative rather than correlative mechanisms of AD [131]. Nevertheless, lessons have been learnt: more research needs to be carried out on identifying epitopes of targeted antigens to improve the accuracy and effectiveness of antibody-based immunotherapy.

2 RESEARCH AIMS

The overall aims of this Ph.D. project were to uncover the mysteries of asparagine deamidation, its toxicity and repair mechanism, thus finding a promising way to fight isoAsp, which can help with the early diagnostics of AD and other NDDs. More specifically, the aims can be described as follows:

Aim 1. To obtain and characterize a monoclonal antibody against isoAsp in HSA, and establish the normal range of isoAsp levels in blood HSA (**Paper I**).

Aim 2. Using the obtained mAb from Aim 1, to investigate deeper the link between isoAsp in blood and AD (**Paper II**).

Aim 3. To study the relationship of isoAsp in blood with other NDDs, especially in early disease stage, and to assess the isoAsp prospects in clinical diagnostics (**Paper III**).

Aim 4. To identify enzymes in human cells with possible succinimide or isoaspartyl ammonia ligase activity (**Paper IV**).

3 MATERIALS AND METHODS

3.1 SAMPLE INFORMATION

3.1.1 Healthy plasma samples in Paper I

In Paper I, plasma samples from a 100-person strong cohort of healthy blood donors were obtained from ProMedDx Limited Liability Company. The samples were collected under a clinical study that had been reviewed by an Institution-al/Independent Review Board (IRB) and/or independent Ethics Committee (IEC) according to the local regulations.

3.1.2 Plasma samples in Paper II

The patients with AD enrolled in Paper II from the Amsterdam Dementia Cohort Biobank were diagnosed according to the criteria of the National Institute on Aging-Alzheimer's Association (NIA-AA) Research Framework [146]. Clinical data was collected through face-to-face interviews by cognitive disorder specialists. Healthy controls at similar ages without cognitive problems were recruited from the Dutch Brain Research Registry. Demographic data included age and sex. For AD patients (except two subjects), the mini-mental state examination (MMSE) was scored. The CSF levels of Aβ42, t-Tau and p-Tau were measured by the Innotest and Elecsys assays [147]. All samples were collected under the declaration of Helsinki with informed consent given to the research participants. The information of both AD and healthy groups was blind to those who processed the samples.

3.1.3 Plasma samples in Paper III

Patients (n = 100: AD, 20; VaD, 20; FTD, 20; PD, 20; MCI, 20) in the study were recruited from the Huashan Hospital of Fudan University (Shanghai, China). Matched healthy controls (n = 40) were recruited from the Chinese Alzheimer's Biomarker and LifestylE (CABLE; Qingdao, China) study as previously described [148-150]. All procedures conformed to the tenets set forth by the Helsinki Declaration. All participants or legal guardians gave their written informed consent. Ethics approval was received from the institutional review boards of each participating center.

General cognitive tests including Mini-Mental State Examination (MMSE) and Montreal Cognitive Assessment (MoCA) were performed by neuropsychological professionals blinded to the study design and subsequent procedures. Some other tests critical for diagnosis like Clinical Dementia Rating scale, Activities of Daily Living, the Unified Parkinson's Disease Rating Scale, and Frontal Behavioral Inventory were also performed. Diagnoses were made by experienced neurologists who were unaware of the research procedures. AD dementia was diagnosed according to the National Institute of Neurological and Communicative Disorders and Stroke and Alzheimer's Disease and Related Disorders Association (NINCDS-ADRDA) criteria [151], as well as the NIA-AA research framework [152]. All patients with AD dementia had strong PET evidence of the disease or CSF-confirmed Aβ-positive pathology. VaD was diagnosed according to the National Institute of Neurological Disorders and Stroke and the Association Internationale pour la Recherche et l'Enseignement en Neurosciences (NINDS-AIREN) criteria [153]. FTD was diagnosed according to the revised criteria set forth by the International Behavioral Variant of FTD Criteria Consortium [154]. PD was diagnosed according to the clinical criteria set forth by the International Movement Disorders Society

(MDS) in 2015 [155]. MCI was diagnosed when there was objective evidence of cognitive decline while no significant evidence of impaired social or self-care ability. Healthy individuals recruited in the study were required to be matched to the patients with AD in terms of age and sex. In addition, all controls had an MMSE score > 24 at the screening visit and no signs of cognitive decline, thus not meeting the criteria for MCI or any NDDs.

3.2 ARTIFICIAL AGING OF HSA AND A SYNTHETIC PEPTIDE

To artificially deamidate HSA, the HSA protein (Sigma Aldrich) was incubated in Tris buffer at pH 8.5 and 60 °C for 7, 14, 28 and 42 days. After digesting the artificially aged and totally fresh HSA (aHSA and fHSA, respectively) by a mix of the enzymes Lys-C and trypsin, we desalted the peptides and analyzed them by LC-MS/MS with electron transfer dissociation (ETD), which provides an isoAsp-specific fragment [32]. Then we identified the isoAsp-containing peptides, quantified the peptide abundances by our home-made software Quanti [33] and calculated the isoAsp occupancy in the Asn-containing peptides as a function of ageing duration (**Paper I, II, IV**). The synthetic peptide LVGNGVL (SynPeptide) was incubated in the same Tris buffer (pH 8.5) at 50 °C for 18 days. The aged peptide was then analyzed by LC-MS/MS (**Paper IV**).

3.3 DEVELOPMENT OF MABS AGAINST THE "ISOASP METER" IN HSA

3.3.1 Generation of mAbs

After the peptide with the highest rate of isoAsp occupancy increase during the ageing process was chosen, its variants with Asn, Asp and isoAsp were synthesized. Hybridoma clones expressing murine mAbs specific to the isoAsp peptide but not to Asn or Asp peptide were then produced by The Russian Research Center of Molecular Diagnostics and Therapy. The clones 1A2 and 1A3 showing the highest specificity were selected for further investigation. In order to find the best method for isoAsp level quantification, we tested the specificity and sensitivity of indirect ELISA (via primary and secondary antibodies) and sandwich ELISA (via capture, detection and secondary antibodies) using chemiluminescence and absorbance for detection, and chose indirect ELISA as the most suitable method showing the highest signal to noise (S/N) ratio (**Paper I, II**).

3.3.2 Indirect ELISA

The antigens aHSA (≈60% isoAsp) and fHSA (~0% isoAsp) were diluted to 10 µg/mL by Phosphate Buffered Saline (PBS) (Cytiva). The 96-well white opaque polystyrene plates (Thermo Scientific) were coated with 50 µL/well of the aHSA and fHSA diluted in PBS and incubated at room temperature for 2 h. Plates were washed in 300 µL/well PBS containing 0.05% Tween-20 (PBST, Sig-ma-Aldrich) three times and shaken dry. The vacant sites were blocked with 200 µL/well 10% skim milk powder (Sigma-Aldrich) in PBST at 4˚C for overnight and washed with PBST as above. Then 50 µL/well of mAb as primary antibody in blocking buffer was added and incubated at room temperature for 2 h. After washing with PBST, a goat anti-mouse IgG Conjugated to Horseradish Peroxidase (Jackson Immuno

Research) was used as secondary antibody and incubated at room temperature for 2 h. Working solution (100 µL/well) was prepared according to the SuperSignal ELISA Pico Chemiluminescent Substrate protocol (Thermo Scientific), and chemiluminescence intensities were measured immediately by the luminometer Tecan Infinite M200 Pro (Tecan) (**Paper I, II, III**).

3.3.3 Characterization of mAbs

The DNA sequences of variable regions in both 1A2 and 1A3 mAbs were analyzed independently by two companies, Fusion Antibodies and Absolute Antibody. Verification of the amino acid sequences of 1A3 mAb was performed independently by Peaks AB and Rapid Novor Inc. Kinetics of the interaction between 1A3 mAb and aHSA were measured by ProteoGenix using the Biacore T2000 SPR biosensor (Cytiva). Paratope mapping was conducted via Hydrogen-Deuterium Exchange Mass Spectrometry (HDX-MS, Biomotif). The effects of deglycosylation on 1A3 specificity were determined by indirect ELISA after the digestion of five enzymes from the glycoprotein deglycosylation kit (Sigma-Aldrich). To study the isotype effect on specificity, another mAb 1A3* was produced by Absolute Antibody with the same variable region sequences as 1A3, but of a different IgG isotype (IgG2b) (**Paper I**).

3.4 QUANTIFICATION OF ISOASP LEVELS IN PLASMA SAMPLES

On each 96-well plate, 50 donor samples were analyzed with indirect ELISA described above together with calibration samples containing 0%, 0.10%, 0.30%, 0.60%, 1.20% and 2.40% isoAsp obtained by mixing fSHA (presumed to have 0% isoAsp) with aHSA (60% isoAsp). For each 96-well plate independently, a linear or second-order polynomial calibration curve was then fitted to the calibration datapoints, and the data of tested samples were converted to % isoAsp. The analysis was performed in 3 replicates (**Paper I, II, III**).

3.5 SIZE EXCLUSION CHROMATOGRAPHY ANALYSES OF FHSA, AHSA AND PLASMA SAMPLES

The SEC analyses were performed on an UltiMate 3000 RSLC-system (Thermo Fisher Scientific) equipped with a variable wavelength detector. The fHSA and aHSA samples were prepared at concentration of 5 mg/mL in PBS, while the plasma samples were diluted to 20 mg/mL in PBS. The UV absorption of each sample was recorded for further comparison analyses. The fractions of aHSA monomer and aggregates were collected to test their isoAsp levels by indirect ELISA (**Paper II**).

3.6 MEASUREMENT OF THE BINDING CAPACITY OF AHSA AND FHSA WITH Aß AND P-TAU

To verify that deamidated HSA has a reduced ability to bind Aß, we incubated Aß 1-42 (Abcam) with aHSA and fHSA for 2 h at 37 °C and then performed fractionation by SEC. The anti-Aß 1-42 mAb (Sigma Aldrich) was then used in indirect ELISA to quantify the amount of

Aß in each fraction diluted to the same protein concentration. A similar experiment was performed with p-Tau. The recombinant p-Tau (Sigma Aldrich) was incubated with aHSA and fHSA for 2 h at 37 °C and then the antigen-antibody complexes were purified via the 100-kD Amicon Ultra Centrifugal filters (Merck). The complexes of p-Tau with HSA were diluted to 5 ug/mL and then quantified by indirect ELISA using monoclonal antibody against p-Tau at Ser-396 (Thermo Fisher Scientific) as the primary antibody. Molecular dynamics simulations of aHSA and fHSA were performed to validate the HSA structural changes upon deamidation and identify the potential sites of HSA binding with Aß [156] (**Paper II**).

3.7 DETERMINATION OF ANTI-AHSA ANTIBODY LEVELS IN BLOOD

3.7.1 Melon gel purification

The IgGs were purified from plasma samples by the Melon Gel IgG Purification Kit (Thermo Fisher Scientific) according to the manufacturer's protocol. The protein concentration was measured by BCA Protein Assay Kit and the purified IgGs were stored at -80 °C until further use (**Paper II, III**).

3.7.2 Indirect ELISA on anti-aHSA antibodies

The 96-well opaque white polysterene plates were incubated with 50 μL of 5 μg/mL aHSA (≈60% isoAsp) at room temperature for 2 h. Plates were rinsed thrice between steps with PBST. After incubating with blocking buffer at room temperature for 2 h, 50 μL purified IgG from each plasma sample (diluted to 800 ng/mL in blocking buffer) was added respectively at 4 ℃ for overnight, followed by incubating with 50 μL secondary antibody - Goat anti-Human IgG (H+L) Secondary Antibody conjugated with HRP (Thermo Fisher Scientific) at room temperature for 2 h. The chemiluminescence was measured immediately after adding the working substrates as above. The data were normalized via dividing the intensity of each sample by the average intensity of each row and column (**Paper II, III**).

3.8 PROTEIN SUCCINIMIDE/ISOASPARTATE AMMONIA LIGASE (PSIAL) ACTIVITY EXPERIMENTS ON "AGED PEPTIDE"

3.8.1 Determination of PSIAL activity in HCT 116 cell lysate

One million HCT 116 cells (ATCC, p = 6) were harvested and washed with cold phosphate-buffered saline (PBS) (Cytiva) three times. The cell pellet was dissolved in PBS buffer supplemented with EDTA-free protease inhibitor (Roche) and phosphatase inhibitor (Roche), snap-frozen in liquid nitrogen and thawn at room temperature. After repeating the "freeze and thaw" procedures for 3 cycles, the cell suspension was centrifuged at 14,000 × g and the supernatant was collected as cell lysate. The mixture in six replicates were prepared with 20 μL of each component in PBS: 10 μM "Aged peptide", 1 mg/mL cell lysate, 100 μM ATP, together with nitrogen donor ($_{L}$-Gln or $_{D}$-Gln) and S-adenosylmethionine (SAM) with different concentrations (as shown in Fig 2a). Three replicates were incubated at 37 °C for 4 h, while the rest replicates were incubated at 4 ℃ for 4 h as controls. All samples were filtered through the Amicon Ultra 3 kDa filter (Millipore) and the filtrate was analyzed by LC-MS/MS. The fold-

change α characterizing the PSIAL activity was calculated for each sample as the relative abundance of the Asn form (P1) in 37 °C incubation versus 4 °C.

3.8.2 Comparison of PSIAL activity among different cell lines

Cell lysate from different cancer cell lines (A498, RKO, HCT116, A549, MCF-7, and HT29) in the same passage (p = 6) was extracted in six replicates by the above procedures, and 1 mg/mL of each cell lysate was incubated with the mixture as above. The fold-change α was calculated for each cell lysate.

3.8.3 Comparison of PSIAL activity among subcellular fractions

The five subcellular fractions (cytoplasmic, membrane, nuclear, chromatin-bound nuclear, cytoskeletal) were extracted from HT29 cell lysate by Subcellular Protein Fractionation Kit (Thermo Fisher Scientific) according to manufacturer's instructions in six replicates. Then 1 mg/mL of different fractions were incubated respectively with the mixture of 10 μM "Aged peptide", 100 μM $_{L}$-Gln, 100 μM SAM, 100 μM ATP similarly to the procedures above and the fold-change α was calculated for each fraction.

3.9 THERMAL PROTEOME PROFILING-TEMPERATURE RANGE (TPP-TR) EXPERIMENTS

To determine which proteins specifically interact with a short isoAsp-containing peptide, the thermal proteome profiling-temperature range (TPP-TR) experiments were performed according to the reported method [157]. In short, the specific melting temperatures for each protein from the "treatment" and "control" samples were compared. Here, the peptide GisoAspGisoAspG (SynPeptide) was used as a "drug" and GDGDG (SynPeptide) as a "control" to treat the HCT116 cells. The other procedures were followed as previously described . The temperature shift of each protein was calculated, as well as the *P* values between two groups. For proteins with a p-value less than 0.05, we generated the score using the formula:

Score = $-|\text{Median}\triangle T| \times \text{Log}_{10}$ (*P* Value of $\triangle$T).

3.10 PSIAL ACTIVITY EXPERIMENTS ON "AGED HSA"

The 0.1 mg/mL aliquot of "Aged HSA" in eight replicates was mixed with 1 mg/mL HT29 cell lysate, 100 μM SAM, 100 μM ATP and 100 μM Nitrogen donor (Amide-^{15}N-enriched Gln, Amine-^{15}N-enriched Gln or normal Gln), and each component was prepared in 20 μL PBS. After incubating 4 replicates of each sample at 37 °C and the rest replicates at 4 °C as controls for 4 h respectively, the samples were subjected to a nano-LC separation using Ultimate 3000 connected in-line with a Fusion Orbitrap mass spectrometer (both - Thermo Fisher Scientific). Peptide separation was performed on a 50 cm long EASY spray column (PepMap, C18, 3μm, 100Å) with a gradient of 5–30% B in 75 min, 30–95% B in 5 min (Solvent A: water with 2% acetonitrile and 0.1% formic acid and Solvent B: acetonitrile with 2% water and 0.1% formic acid). Precursor ion fragmentation was performed with consecutive higher-energy collision dissociation (HCD; collision energy: 27%, resolution 70,000, AGC target 5.0e4, maximum

injection time 200 ms) and electron-transfer/higher-energy collision dissociation (EtHCD; collision energy: 40%, resolution 17,500, AGC target 5.0e4, maximum injection time 200 ms). The relative mass shift was monitored as a centroid of the mass distribution for an isotopic cluster of the MH^+ molecular ion encompassing its monoisotopic peak M as well as two subsequent isotopic peaks M + 1 and M + 2, as shown in the formula:

$$\text{Relative Mass Shift (\%)} = \frac{Intensity\ of\ (M+1) + 2 \times Intensity\ of\ (M+2)}{Intensity\ of\ M} \times 100\%.$$

4 RESULTS AND DISCUSSION

4.1 PAPER I. FIRST IMMUNOASSAY FOR MEASURING ISOASP IN HSA

In Paper I, we obtained and characterized a monoclonal antibody against isoAsp in a structurally and functionally important domain of HSA.

First, via MS/MS analysis of artificially aged HSA (aHSA) we found that the peptide "LVNEVTEFAK" exhibited the highest deamidation rate and its isoAsp occupancy reached a plateau at 63% after 28-day artificial deamidation at 60 ^{o}C and pH 8.5 (**Figure 6A, B**). In the native structure of HSA protein, this peptide is located in the position exposed to the solvent (**Figure 6C**), which explains its high isoAsp formation rate and it being prone to bind with antibodies. Furthermore, this peptide is located in domain I, the binding affinity of which to Aß monomer is the strongest among the three domains. Such binding can hamper the structural transformation of Aß42 protofibrils to fibrils. Thus, this peptide was chosen to be the "isoAsp meter" representing the isoAsp occupancy in the whole HSA molecule. Against this peptide in aHSA, two hybridoma clones were obtained from collaborators, producing murine mAbs 1A2 and 1A3, which showed the highest specificity. We compared different types of ELISAs with different settings (**Table 2**) and discovered the highest sensitivity in the indirect ELISA using chemiluminescence for detection. The signal to noise ratio (S/N) reached 39.9 at 6% isoAsp and 4.3 at 0.6% isoAsp. Thus, this method was chosen for further analyses. In terms of the signal ratio of aHSA versus fresh HSA (fHSA), 1A3 showed much higher specificity compared to 1A2, and the S/N of 1A3 reached ≥ 3 already at 0.1% isoAsp occupancy (**Figure 6D**).

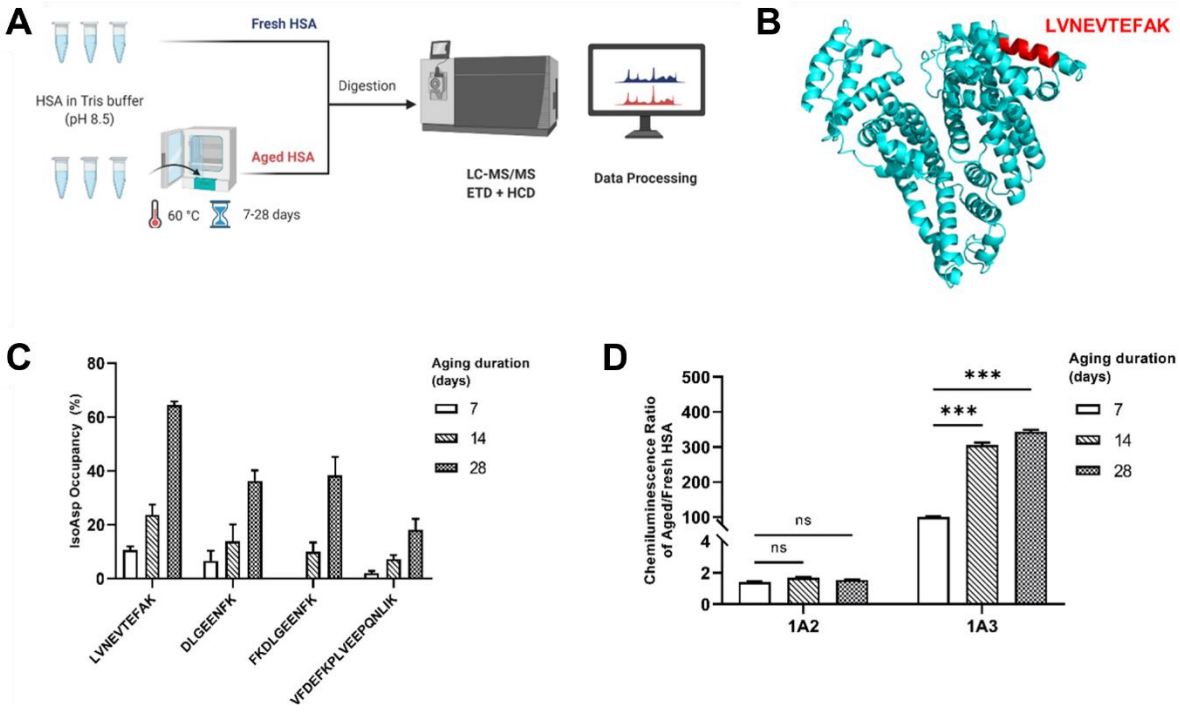

Figure 6. Development of the indirect ELISA against isoAsp in HSA. (A) Discovery of the "IsoAsp meter" peptide for measuring isoAsp in HSA. Artificially deamidated HSA was digested, with the peptides analyzed by LC-MS/MS with ETD and HCD fragmentation and label-free peptide quantification. (B) Changes of the isoAsp occupancy in Asn-containing HSA peptides over aging duration. (C) Location of the peptide LVNEVTEFAK in the structure of HSA monomer. (D)

Comparison of the specificity between 1A2 and 1A3 mAbs against HSA artificially aged for 7–14–28 days. The signal ratio of aged/fresh HSA provided the dynamic range related to the mAb specificity. ****$P < 0.0001$.

Table 2. Comparison among different ELISA methods.

	Indirect ELISA		**Indirect Sandwich ELISA**		
Plate	White Polystyrene	Copper-Coated	White Polystyrene	White Polystyrene	Copper-coated
Blocking buffer	10% Milk in PBST				
Capture antibody	N/A		15C7 anti-HSA mAb	1A3 mAb	1A3 mAb
Primary/Detection antibody	1A3 mAb		1A3 mAb	1A2 mAb	1E1 anti-HSA mAb
Secondary antibody	Peroxidase AffiniPure Polyclonal Goat Anti-Mouse IgG + IgM (H + L)				
Detection	Chemiluminescence	Absorbance	Chemiluminescence	Chemiluminescence	Absorbance
S/N at 6% isoAsp	39.9	12.1	0.8	0.6	0.8
P value	$< 10^{-5}$	$< 10^{-5}$	7.0×10^{-3}	$< 10^{-5}$	$< 10^{-5}$
S/N at 0.6% isoAsp	4.3	3.6	N/A		

More fundamentally, the nucleotide sequencing results demonstrated the difference of only one amino acid in both V_H and V_L domain between 1A2 and 1A3, which was validated by subsequent amino acid sequencing. The replacement of Ser by Ile-51 in the V_H and Leu-60 in the V_L enhanced the mAb specificity against isoAsp by three orders of magnitude. Another difference between the two mAbs was the Ig isotype: 1A2 was of IgM isotype and 1A3 – IgG3 isotype. Besides, the kinetics analysis revealed a K_D of 1A3 interacting with aged HSA of 2.09 $\times 10^{-8}$ M, indicating an above-middle binding affinity (**Figure 7A**, **Table 3**). Paratope mapping by HDX-MS/MS showed that deuterium incorporation reduced most in the region "FIRNKANGYTTE" upon ligand binding, confirming the critical role of Ile-51 for 1A3 specificity (**Figure 7B-C**).

Table 3. Kinetic binding parameters of the interaction of 1A3 with aHSA.

Antibody-Antigen	k_a **($M^{-1}s^{-1}$)**	k_d **(s^{-1})**	K_D **(M)**
1A3-aHSA	$2.6 \pm 0.5 \times 10^{-5}$	$5.3 \pm 0.4 \times 10^{-3}$	$2.1 \pm 0.3 \times 10^{-8}$

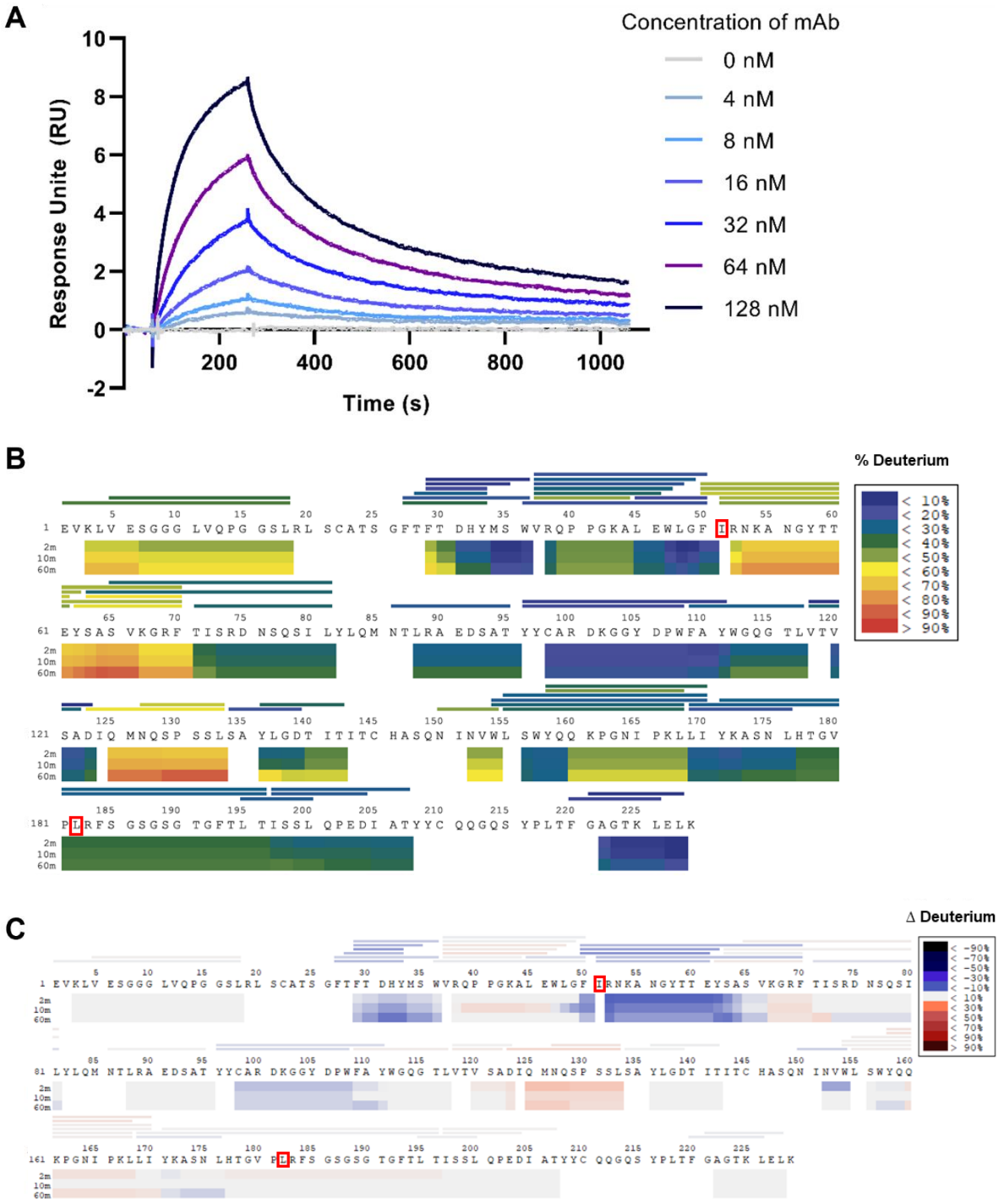

Figure 7. Characterization of binding interface between 1A3 mAb and aHSA. (A) The sensorgram of 1A3-aHSA interaction at different mAb concentrations. (B) The coverage of the 1A3 sequence by reporter peptic fragments (horizontal lines) in HDX MS analysis and the background deuterium incorporation (horizontal bars). (C) The differential deuterium incorporation between the mAb/aHSA complex and the mAb alone. Negative values (in blue) represent protection/stabilization while positive values (in red) indicate destabilization.

Our amino acid sequencing also revealed the glycosylation position on 1A3, and deglycosylation did not decrease the specificity of 1A3 dramatically – it was diminished most by ß1,4-galactosidase (**Figure 8A)**. The V_H and V_L sequences of 1A3 were incorporated into 1A3* mAb of the IgG2B isotype. The specificity of 1A3* was greatly reduced compared to

that of 1A3, but still much higher than that of 1A2 (**Figure 8B)**. In the end, we applied the developed indirect ELISA to quantify the plasma isoAsp levels in 100 healthy donors. The results revealed a normal distribution, and the average isoAsp level was 0.74% ± 0.13% in two independent experiments (**Figure 8C-D**).

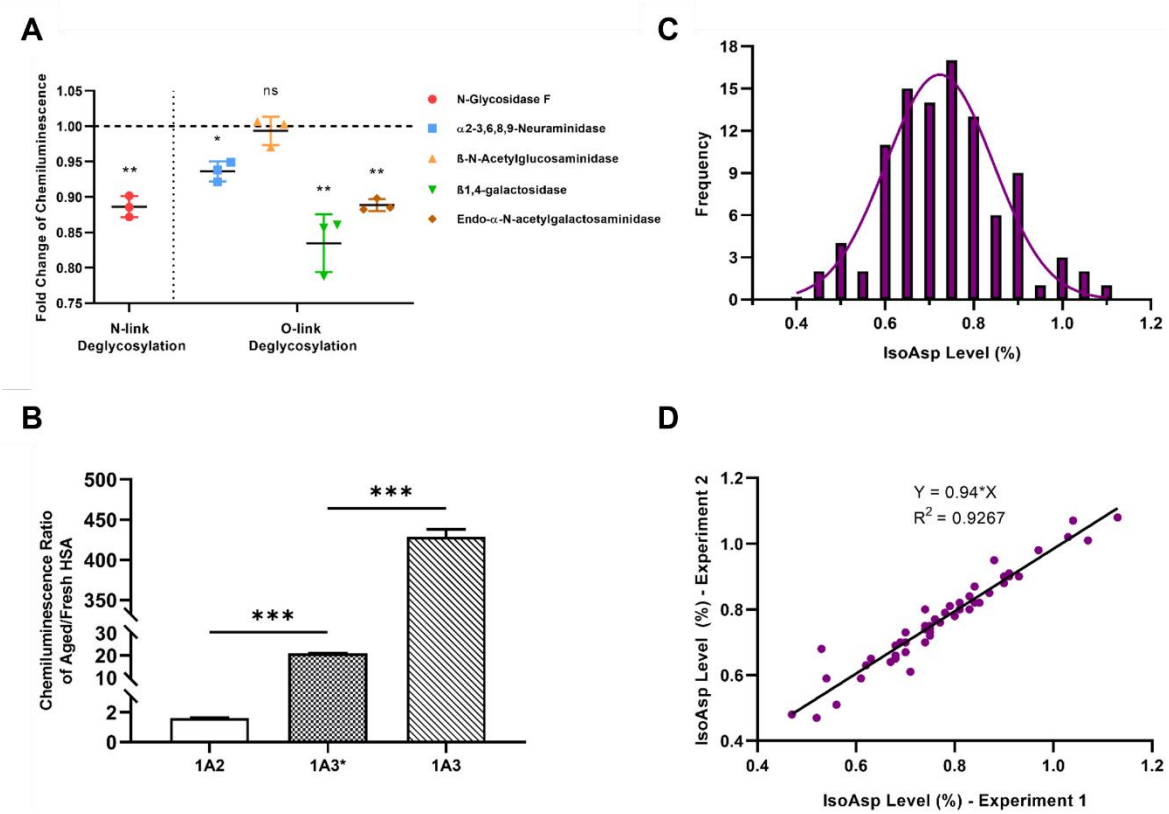

Figure 8. The application of 1A3 mAb in indirect ELISA for determination of isoAsp in blood HSA. (A) The changes in 1A3 specificity to aHSA after deglycosylation by five different galactosidases * $P < 0.05$; ** $P < 0.01$; ns: not significant. (B) The comparison of specificity to aHSA versus fHSA among 1A2, 1A3* and 1A3 mAb, where 1A3* has the same variable region sequences as 1A3 but of a different IgG isotype; *** $P < 0.0001$ (C) The distribution of isoAsp occupancies in HSA measured in 100 blood plasma samples from healthy individuals, obtained using linear calibration. (D) Comparison between the ELISA results of 50 blood plasma samples measured using 1A3 antibody with a two-week interval.

In conclusion, we obtained and characterized a mAb sensitive to isoAsp in HSA, the first of its kind, and based on that mAb developed an ELISA demonstrating good specificity and sensitivity in quantification of the isoAsp level in blood, which we can use for studying the link between isoAsp and AD.

4.2 PAPER II. TESTING THE LINK BETWEEN ISOASP AND AD ETIOLOGY

The SEC analysis of aHSA and fHSA revealed different quaternary structures of these two forms of HSA. The fHSA showed a main peak representing the monomer of HSA, a smaller satellite representing the dimer, and a much smaller oligomer peak, while aHSA produced two obvious peaks (**Figure 9A**). The earlier peak corresponds to the HSA aggregates composed of

no less than eight molecules, with a higher isoAsp level by 3 times compared to the monomers (**Figure 9B**). Consistent with HSA aggregation, we discovered a few of the plasma samples to be cloudy, with visibly insoluble depositions. Further SEC analyses of plasma samples confirmed a significantly increased HSA aggregate/monomer ratio in AD blood. More specifically, the largest difference of UV absorbance between AD and Healthy occurred at Peak 1, retention time (RT) = 6.3 min (**Figure 9C**), which corresponds to the RT of aHSA aggregates (**Figure 9B**). The absorbance ratio dropped to the lowest (< 1) at Peak 2, RT = 9.5 min (**Figure 9C**), corresponding to HSA monomers. The absorbance ratios of Peak 2/1 in the two groups were plotted (**Figure 9D**), while the respective receiver operating characteristic (ROC) curves were drawn (**Figure 9E**). The corresponding areas under the curve (AUCs) are from 0.86 at RT = 6.3 min to 0.95 at RT = 9.5 min (**Figure 9E**).

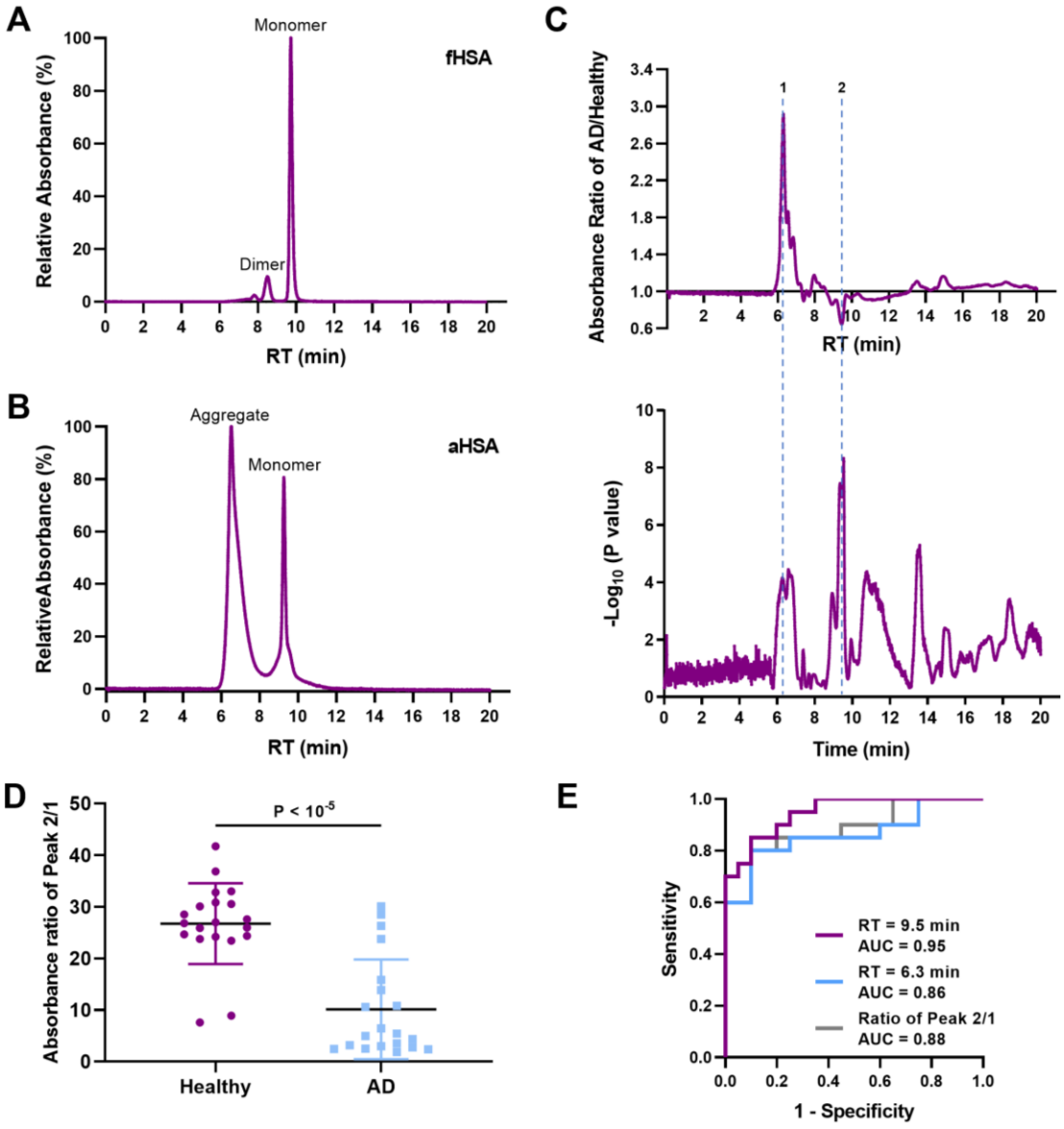

Figure 9. HSA aggregation due to the isoAsp deamidation. The SEC results of (A) fHSA and (B) aHSA. (C) UV absorbance ratio of the AD and Healthy group (Up) and the corresponding *P* values (Down), (D) The ratio of the UV absorbance at Peak 2 (RT = 9.5 min) and Peak 1 (RT = 6.3 min). (E) The ROC curves of the comparisons between the AD and Healthy cohorts.

Among the fractions of fHSA and aHSA separated by SEC, fHSA monomers exhibited the greatest capacity of binding Aß, followed by fHSA dimers, while the monomers of aHSA showed the weakness of such ability, and even worse did the aHSA aggregates – negligible binding capacity toward Aß (**Figure 10B**). Similarly, a modest but significant ($P < .05$) decline was found in the capacity of aHSA binding with p-Tau compared to fHSA (**Figure 10C**). Molecular dynamic simulation of fHSA and aHSA also confirmed the structural deviation of HSA upon deamidation (**Figure 10D**). Intriguingly, the remarkable changing region also overlapped with the Aß binding sites identified computationally (**Figure 10E-F**).

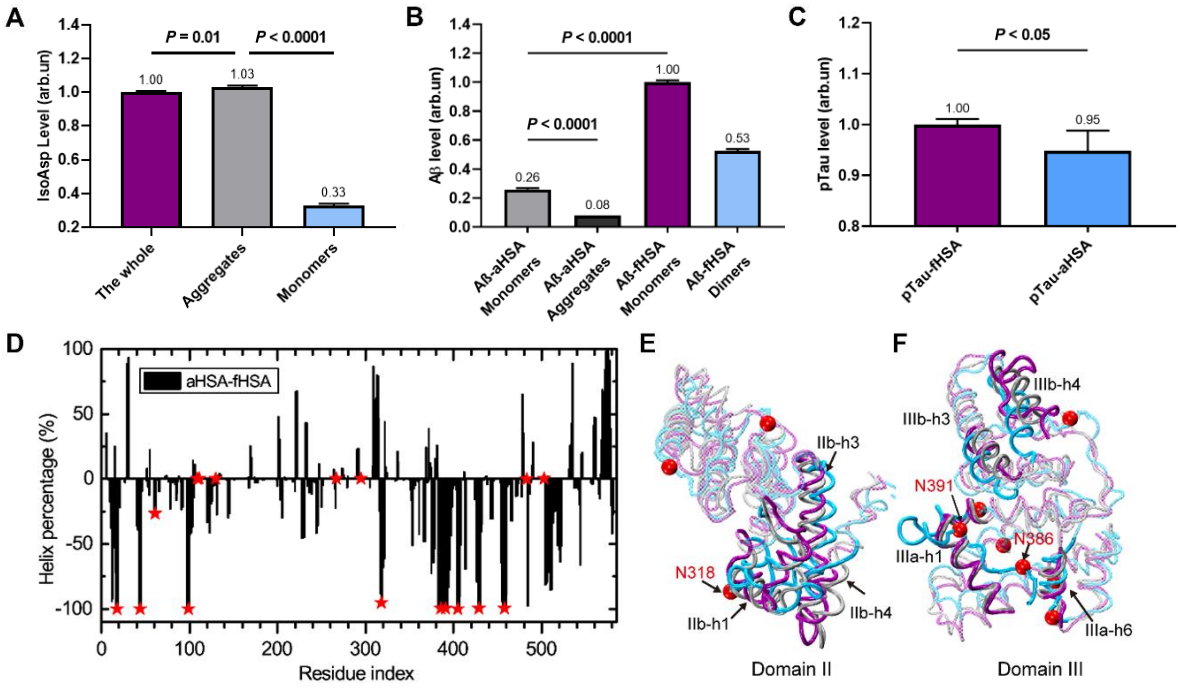

Figure 10. Confirmation of the lower binding capacity of deamidated HSA with Aß and p-Tau. (A) The isoAsp levels in whole aHSA and its fractions of aggregates and monomers. (B) The normalized Aβ level binding with different fractions of aHSA and fHSA. (C) The normalized p-Tau level binding with different fractions of aHSA and fHSA. (D) The difference of the helix percentage in each residue between aHSA and fHSA. Values under unity: the reduction of helix structures in aHSA compared with fHSA. Red stars: the deamidation sites. The superpositions of domain II (E) and III (F) in the final state of aHSA (purple) and fHSA (blue) simulations with the crystal structure (gray). Red spheres: the deamidation sites. Regions with notable structural deviations are opaque while the rest are transparent.

Using LC-MS/MS, we discovered in AD blood elevated levels of isoAsp in HSA compared with healthy controls (**Figure 11 A-B**). This finding was confirmed via the indirect ELISA using our mAb developed in **Paper I**. Interestingly, reduced endogenous anti-aHSA antibody levels were discovered and negatively correlated with the isoAsp levels (**Figure 11 C-D**), indicating the hampered clearance of Aß and p-Tau in AD. We also verified the decreased level of Aß not bound with HSA in AD than that in healthy group (**Figure 11E**), supporting the diminished capacity of aHSA to bind with Aß and p-Tau. The AUCs for both isoAsp and anti-aHSA antibody levels were above 0.8 (**Figure 11F**).

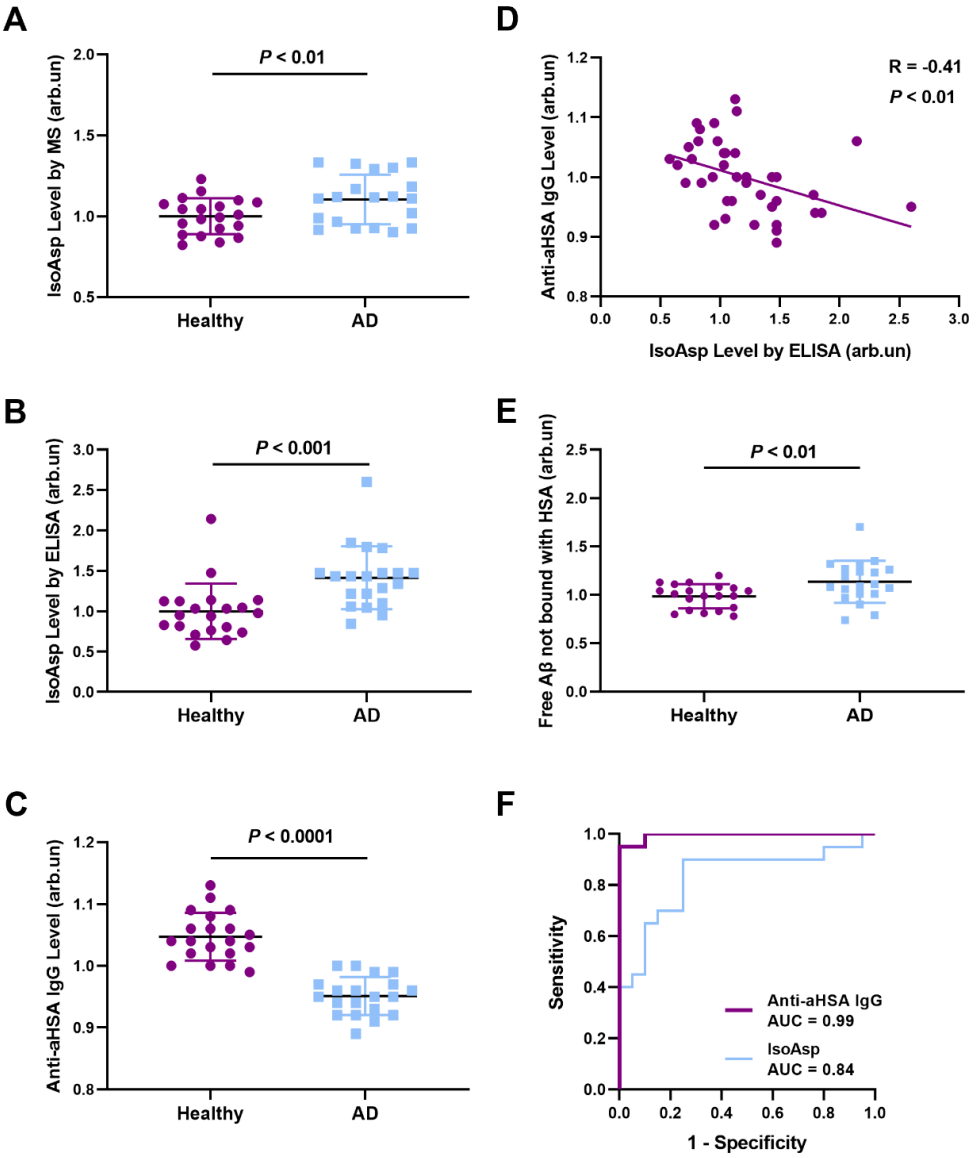

Figure 11. Verification of higher isoAsp content and lower level of anti-isoAsp antibodies in AD blood. (A) The isoAsp levels in the peptide LVNEVTEFAK via LC-MS/MS analysis of Healthy and AD plasma samples. (B) The significantly increased isoAsp levels in AD compared to healthy controls measured by the indirect ELISA in three independent experiments. (C) The anti-aHSA IgG levels detected by the ELISA with aHSA as an antigen bait to capture the IgGs purified from the same cohort. (D) The negative correlation between anti-aHSA IgG level and isoAsp level by ELISA. (E) An increased level of free Aß not bound with HSA in AD blood compared to healthy controls. (F) The ROC curves on the isoAsp levels by ELISA and the anti-aHSA IgG levels.

According to the discoveries above, we updated the isoAsp hypothesis of AD (**Figure 12**) that is formulated as follows: the elevated isoAsp level in HSA results in its partial unfolding and aggregation, and both diminish the capability of HSA to carry its ligands, including Aß and p-Tau, leading to their reduced clearance by the liver and kidneys. Consequently, the enhanced Aß and p-Tau aggregation in the brain increases the AD risk. As isoAsp is somewhat immunogenic, the endogenous antibodies against aged HSA exist for removing isoAsp, and the isoAsp accumulation in AD correlates with reduced levels of such antibodies. In summary,

this hypothesis supports a role for isoAsp build-up in the etiology of AD and offers new avenues for diagnostics, and possibly preventive and therapeutic strategies for AD.

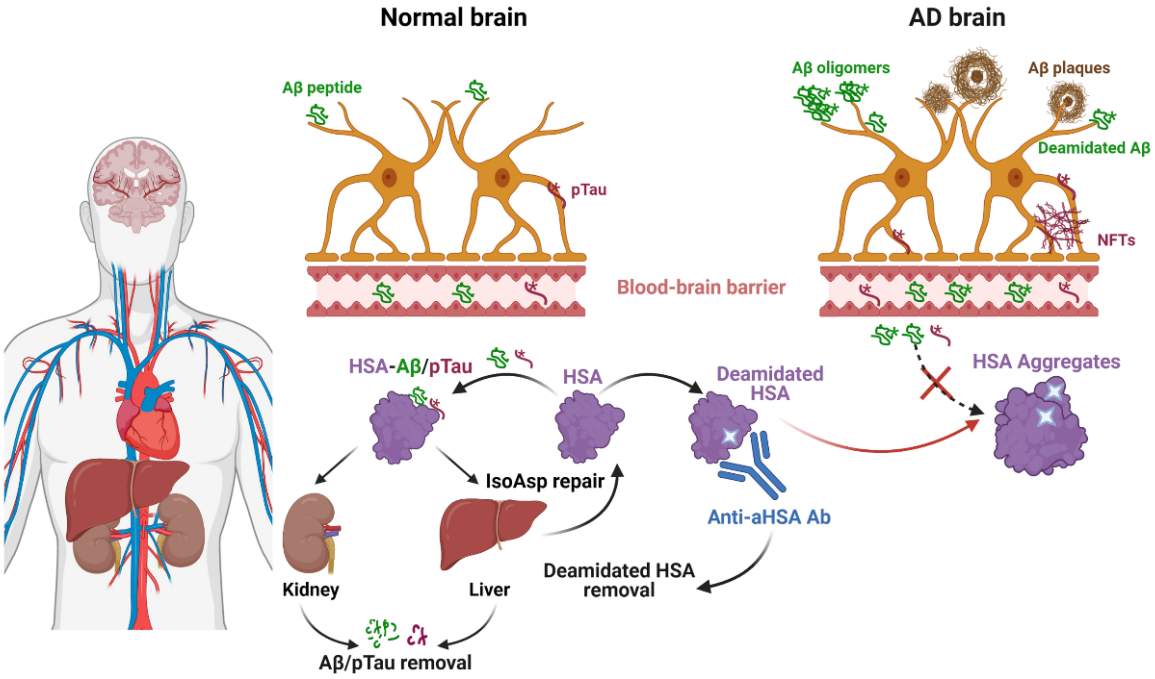

Figure 12. The updated isoAsp hypothesis of AD etiology.

In principle, the main hypothesis suggests that the enhanced protein deamidation may result from the peripheral metabolic disorder in the early stage of AD. A key aggravating factor can be the decreased levels of anti-aHSA antibodies in AD blood that help removing deamidated HSA and thus hindering HSA aggregation. The reason for such decline of the anti-aHSA antibodies could be explained as follows: on one hand, the further deficiency of immune system in patients with AD and other NDDs [158, 159] may reduce the production of antibodies in response to HSA deamidation; on the other hand, the increased levels of isoAsp in blood HSA may simply consume the supply of such anti-aHSA antibodies. These reasons are not mutually exclusive and can act simultaneously. Furthermore, isoAsp in blood proteins can induce inflammation, which is also one of the central mechanisms driving the AD onset. For example, isoAsp-containing fibronectin was found to activate both monocytes and macrophages in mice, inducing the expression of pro-inflammatory cytokines to trigger recruiting circulating leukocytes additionally [160]. Since the increasing isoAsp level in HSA is due to the reduced efficiency in isoAsp repair or clearance, this also suggests an elevated risk of inflammation. Thus, the increasing isoAsp levels could contribute to chronic neuroinflammation, reflected by the reduced levels of blood anti-aHSA antibodies in the long term.

In summary, the results and insights in this paper provide novel ways of diagnosing AD. Since the disruption of Aß and p-Tau clearance occurs ahead of their aggregation, isoAsp biomarkers show a potential in supplementing early diagnostics of AD and other NDDs. Nevertheless, this potential needs to be tested in a larger cohort to determine the sensitivity and specificity of the approach. Also, the predictive capability of isoAsp biomarkers shall be compared with that of other biomarkers currently used in clinics, such as memory test scores, CSF and blood Aß and

p-Tau levels, sizes of Aß plaques or neurofibrillary tangles, etc. Some of these issues were addressed in **Paper III**.

4.3 PAPER III. ISOAP-RELATED BLOOD BIOMARKERS SHOW PROMISE FOR EARLY DIAGNOSTICS OF NEURODEGENERATION

Cohort 1 (CN: 20; AD: 20) validated the results in **Paper II** with a significant increase of isoAsp in HSA and deficiency of IgG against aHSA in AD group compared to controls ($P < 0.0001$). The normalized signals reflecting the isoAsp level in AD plasma HSA were increased by 9% on average ($P < 0.0001$, **Figure 13A**), while the anti-aHSA IgG average signal was reduced by 6% ($P < 0.0001$, **Figure 13B**) with the isoAsp/anti-aHSA IgG ratio being 15% higher in AD ($P < 0.0001$, **Figure 13C**). The diagnostic values of the three above parameters were assessed using ROC curves and the area under the curve (AUC) values (**Figure 13D**). All of the AUCs were above 0.80, suggesting good differentiation between AD and control. We also compared the AUCs of IsoAsp parameters with other plasma biomarkers, and the former significantly surpassed Aß40 and Aß42, but somewhat underperformed NfL, GFAP and p-Tau181 (**Figure 13E**).

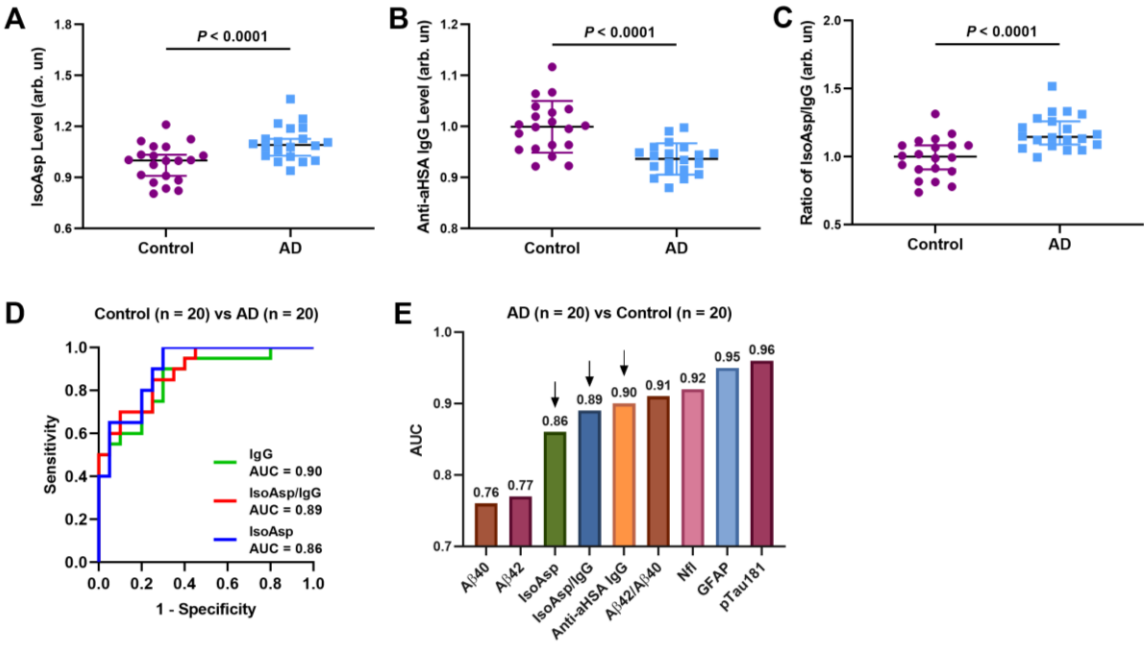

Figure 13. Validating the isoAsp biomarkers in differentiating AD vs Control. (A) IsoAsp levels in HSA are increased, and (B) the anti-aHSA IgG levels are decreased in AD compared to Control; (C) the isoAsp/anti-aHSA IgG ratios are also different. The ROC curves for differentiating AD and controls by (D) IsoAsp in HSA, anti-aHSA IgG and isoAsp/IgG ratio. The comparison of AUCs of all blood biomarkers (E).

Cohort 2 (CN: 20; MCI: 20; VaD: 20; FTD: 20; PD: 20) revealed similar trends comparing controls and subjects with different NDDs: significantly elevated isoAsp levels (by ≥18%, **Figure 14A**) in MCI ($P < 0.001$), VaD ($P < 0.01$) and FTD ($P < 0.001$), and significantly lower anti-aHSA IgG levels (**Figure 14B)** in MCI ($P < 0.001$) and FTD ($P < 0.01$). The IsoAsp/IgG

ratios also showed a significant difference in MCI ($P < 0.001$), VaD ($P < 0.01$) and FTD ($P < 0.001$), with median values ≥ 19% compared to control (**Figure 14C**). No significant difference was observed for PD despite a 9% elevation of the average value, likely due to the large spread of data within the PD group. Collectively, the isoAsp-related biomarkers showed reasonable efficacy (AUC = 0.78..0.83) in diagnosis of other dementia types than controls (**Figure 14D**), and very promising efficacy (AUC = 0.86..0.92) in the stage of mild cognitive decline ahead of dementia diagnosis (**Figure 14E**). More specifically, the IsoAsp/IgG ratio ranked the first among all plasma biomarkers (AUC = 0.92), followed by IgG, p-Tau181 (both AUC = 0.87) and isoAsp (AUC = 0.86) (**Figure 14F**).

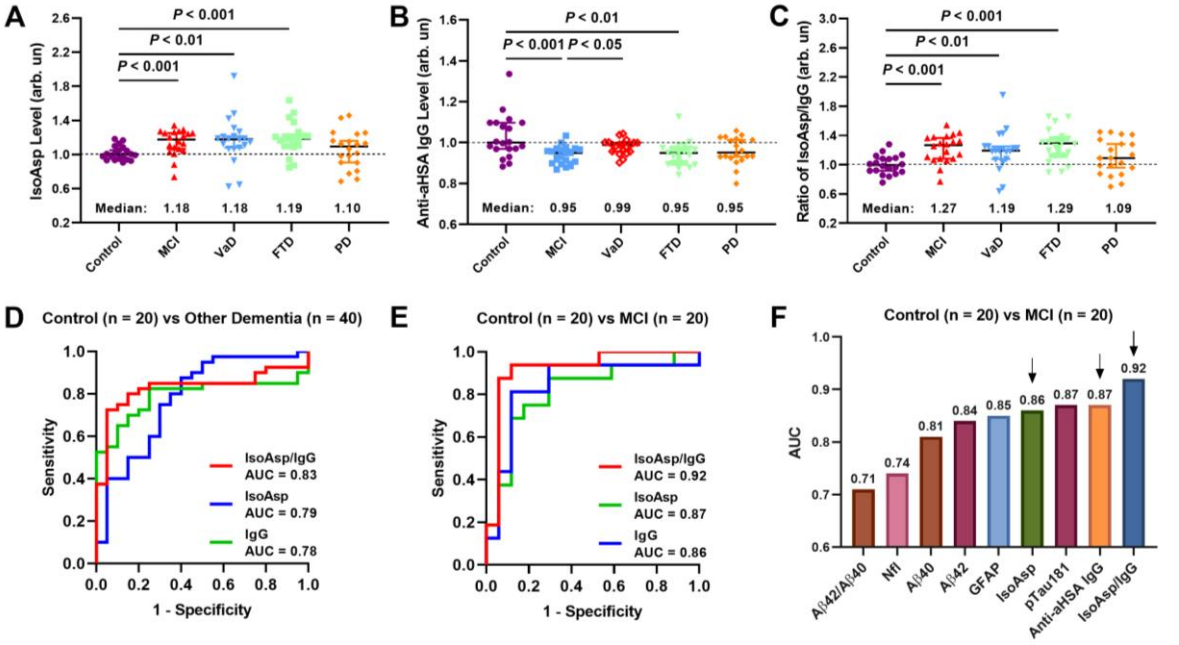

Figure 14. Differentiation among various NDDs and disease stages. (A-C) Distinguishing Control from MCI and Other NDDs (VaD, FTD and PD). The ROC curves for differentiation between (D) Other dementia (VaD and FTD) and control, (E) MCI and control. (F) The comparison of AUCs of all blood biomarkers.

Strong positive correlation was discovered in both cohorts between cognitive scores (MMSE and MoCA) and the anti-aHSA IgG levels ($P < 0.01$), while there was negative correlation between the cognitive scores and the isoAsp levels in plasma HSA as well as IsoAsp/IgG ratio ($P < 0.01$), supporting the link between the isoAsp biomarkers and the early onset of disease pathology (**Figure 15A-F**). In parallel, we found a negative relationship of anti-aHSA IgG with plasma Aß40, Aß42/Aß40 ratio, GFAP and NfL, while both isoAsp and the isoAsp/IgG ratio were positively associated with them. The levels of isoAsp biomarkers were significantly associated with the memory test scores ($P < 0.05$). The most significant finding was the best performance in MCI detection of isoAsp-related biomarkers compared with other blood biomarkers.

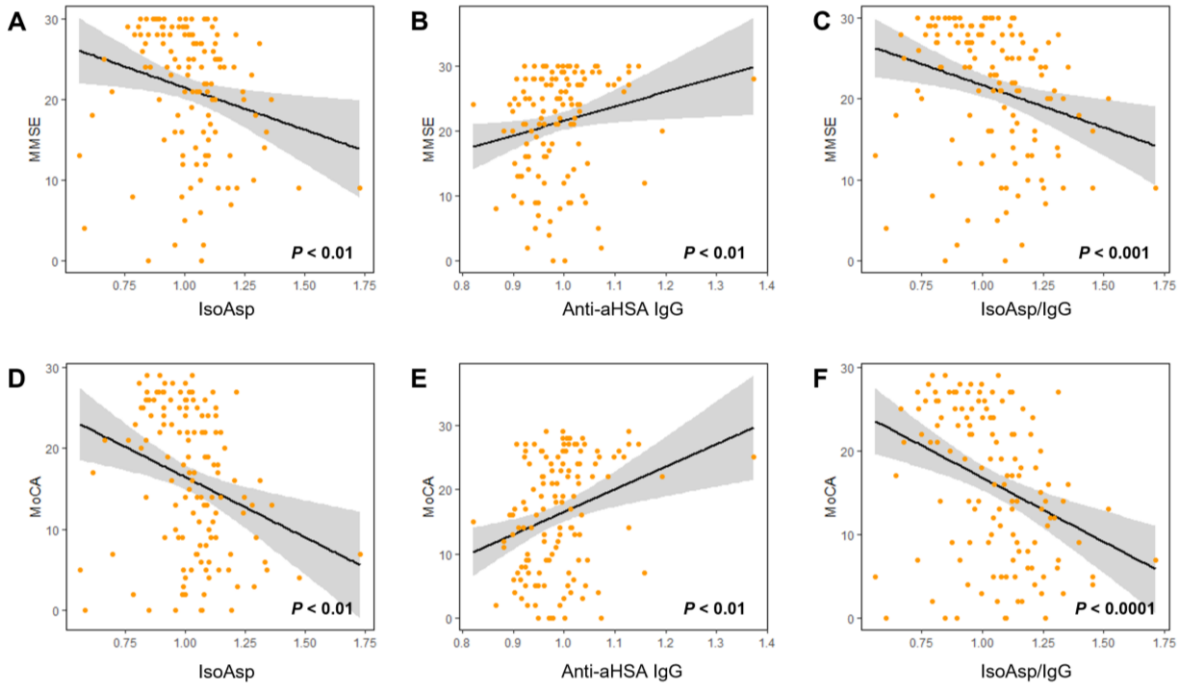

Figure 15. Association of memory scores with isoAsp biomarkers. Linear regression analyses for MMSE score (A-C) and MoCA score (D-F) versus (A, D) IsoAsp in HSA, (B, E) Anti-aHSA IgG, (C, F) IsoAsp/IgG ratio.

According to the previous and current findings in **Paper III**, we propose the following isoAsp mechanism on the initiation of NDDs (**Figure 16**). In a healthy body, spontaneously deamidated HSA is repaired by the enzyme PIMT in liver using SAM as a cofactor; the anti-aged-HSA antibodies in blood remove deamidated HSA, and the newly synthesized HSA molecules restore homeostasis. When in aging the SAM levels become insufficient due to reduced synthesis and increased consumption, PIMT-mediated isoAsp repair diminishes, the isoAsp starts to accumulate in blood proteins, depleting the stock of the native antibodies against isoAsp. This causes reduced removal of deamidated HSA and formation of HSA aggregates. Deamidated and aggregating HSA has a diminished capacity of binding with Aβ, p-Tau, metal ions and other molecules both in blood and CSF, reducing their clearance from brain and contributing to their enhanced aggregation there. It is also plausible that the reduced isoAsp repair and removal concerns brain proteins involved in maintaining cognitive functions. Therefore, the isoAsp in blood acts as a "thermometer" for the state of protein health in general, reflecting both cognitive decline and the onset of non-PD neurodegenerative diseases.

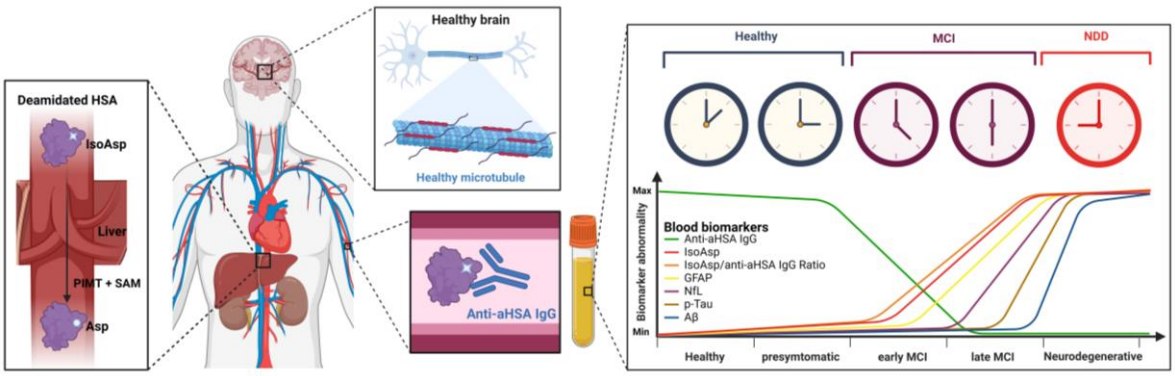

Figure 16. The model connecting the overall state of isoAsp repair/removal in proteins with the onset of neurodegenerative diseases, supporting early disease diagnostics by isoAsp biomarkers.

This study validated previous findings of the important role of blood isoAsp in AD and discovered such a role in other NDDs, but possibly not in PD. An important finding is the excellent performance of these biomarkers, isoAsp, anti-aHSA IgGs, and the isoAsp/anti-aHSA IgG ratio, in early stages of mental decline and a significant correlation with mental scores.

4.4 PAPER IV. FIRST EXPERIMENTAL EVIDENCE FOR REPAIR OF AMMONIA LOSS FROM ASN

Does true repair of Asn deamidation occur in nature? In this paper, we discuss the possibility of a reaction of isoAsp repair to Asn both theoretically and experimentally.

From the theoretical perspective, there are entropy considerations concerning the full repair of isoAsp. Since ammonia (NH_3) concentration is orders of magnitude lower than that of water in the cellular environment [161], spontaneous NH_3 attachment to Succ has lower possibility than water attachment to form (iso)aspartyl residue. However, molecular dynamic simulations revealed that although the conversions of Asn to Succ and Succ to isoAsp involve overcoming large energy barriers, the overall enthalpy change is close to zero [162]. Moreover, microscopic reversibility principle also suggests both direct reaction (NH_3 loss + H_2O attachment) and reverse reaction (H_2O loss + NH_3 attachment) to take place. Therefore, at some isoAsp level and under certain experimental conditions could the equilibrium be reached. Indeed, we discovered that during the artificial deamidation of HSA, the isoAsp level in the partial sequence LVNTEFAK reached around 60%, and this level did not change during the artificial deamidation incubation from 28 to 42 days. Therefore, it is reasonable that both Asn deamidation and its reverse activity are possible via the enzyme(s) we named as protein succinimide/isoasapartate ammonia ligase (PSIAL). The one-step conversion from isoAsp to Asn is possible as well, since one-step Asn deamidation forming isoAsp has been postulated [163].

If PSIAL activity exists in nature, this kind of activity should be active in cells possessing self-renewal characteristics, for example, stem cells, including cancer stem cells. In this paper, we

initiated a search for PSIAL activity evidence and reported its existence based on the promising results.

First, we designed an assay to detect the PSIAL activity on a synthetic short peptide that was artificially deamidated. After incubating the peptide LVGNGVL containing 99.9% isoAsp (**Figure 17A-B**) with cell lysate and other cofactors (SAM, ATP and a nitrogen-rich amino acid), the components with less than 3 kDa were filtered for LC-MS/MS analysis (**Figure 17C**). The abundance of peptide LVGNGVL in three different forms (with Asn, Asp and isoAsp, **Figure 17B**) was determined by label-free proteomics, and the fold-change α representing the relative abundance of the Asn form in 37 ℃ incubation versus 4 ℃ incubation was calculated for measuring the PSIAL activity. In the first batch of experiments on HCT116 cell lysate, the highest PSIAL activity was spotted when using 100 μM L-Gln and 100 μM SAM as the cofactors ($\alpha = 7.8 \pm 0.8$; **Figure 17D**). Under the same conditions, we found that HT29 showed the most significant PSIAL activity among six different cancer cell lines (**Figure 17E**). To localize the PSIAL activity, we further separated the HT29 cell lysate into membrane, cytoplasmic, cytoskeletal, nuclear, and chromatin-bound fractions. The results (**Figure 17F**) demonstrated the highest PSIAL activity in the cytoplasmic fraction ($\alpha = 1.9 \pm 0.2$) and the lowest one in the nuclear fraction ($\alpha = 1.2 \pm 0.1$).

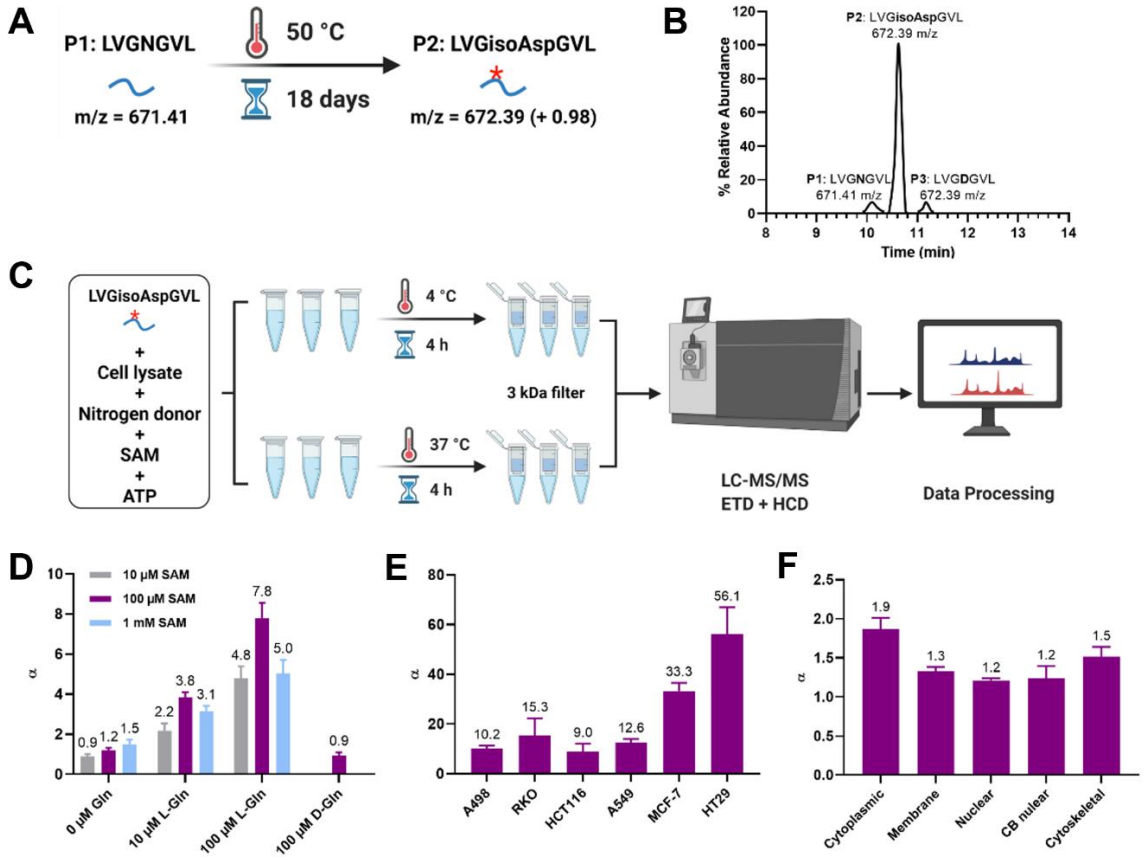

Figure 17. Discovery of PSIAL activity on synthetic isoAsp-containing peptide. (A) Artificial deamidation of the synthetic peptide LVGNGVL (P1) to LVGisoAspGVL (P2) via incubation at 50 °C for 18 days. (B) The chromatogram of the aged peptide above in three forms with Asn (P1), isoAsp (P2) and Asp (P3). (C) The scheme of testing PSIAL activity in cell lysate using aged P1 and cofactors. (D) The effects of cofactors (Gln and SAM) with different concentrations on PSIAL activity. (E) Comparison of PSIAL activities among different cancer cell lines by measuring the fold-change α of

the relative abundance of the Asn form of peptide in 37 °C incubation versus 4 °C. (F) Comparisons of PSIAL activities among different subfractions of HT29 cell lysate.

To validate these results, we carried out a second batch of experiments using artificially aged HSA (aHSA) with deamidated polypeptides (**Figure 18A-C**) by incubating it with SAM, nitrogen donors and ATP (**Figure 18 D**). We confirmed the PSIAL activity of HT29 cell lysate on aHSA, and found that amide-^{15}N glutamine gave the largest mass shift as nitrogen donor compared with amine-^{15}N and normal glutamine (**Figure 18E**). Both amine-^{15}N and amide-^{15}N Gln contributed to the reamination, possibly because of the existence of several enzymes for reamination. Moreover, deamidation in general is a relatively slow process, its repair is likely to be slow as well. The slowly acting enzymes may be less specific, since they explore various kinds of molecular configurations over a long period and each has its own specificity. Additionally, the enzyme specificity is usually overestimated, while from evolutionary perspectives they should maintain wide specificity [164]. By thermal proteome profiling [157] experiments, the proteins interacting with deamidated peptide were discovered as potential enzymes with PSIAL activity, and the cytoplasmic aspartate aminotransferase (GOT1) showed the highest score using the formula combining melting temperature shift ΔT and *P* value. The PSIAL activity of recombinant GOT1 protein was validated (**Figure 18F**).

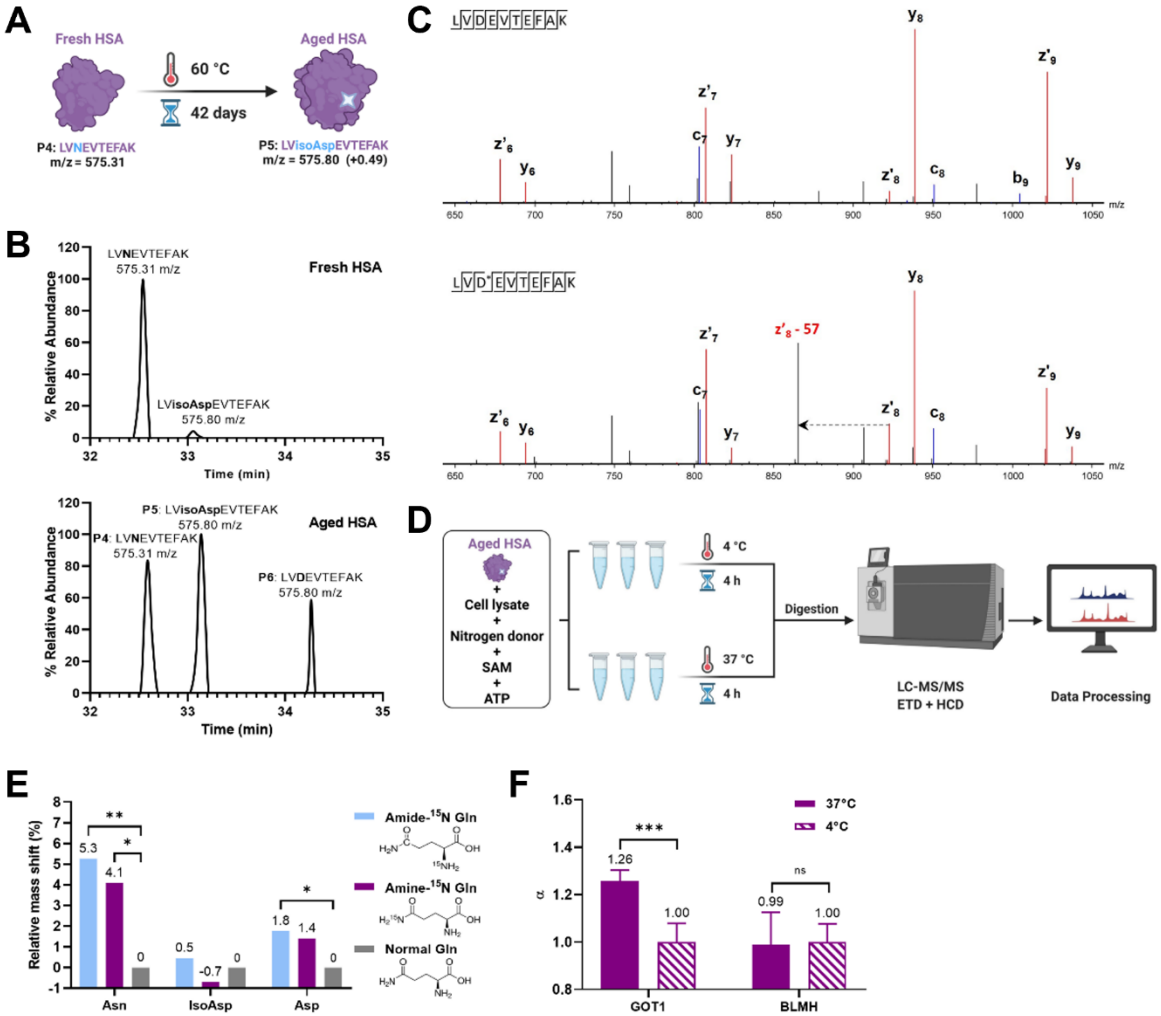

Figure 18. Discovery of PSIAL activity on aged HSA. (A) Artificial deamidation of fresh HSA to aged HSA via incubation at 60 °C for 42 days. (B) The chromatogram of fresh (up) and aged (down) HSA (D* = isoAsp). (C) The ETD MS/MS spectrum confirming the isoAsp presence by the z'_8-57 ion (Up) and its absence in the corresponding peptide with Asp (Down). (D) The scheme of testing PSIAL activity in cell lysate using aged HSA and cofactors. (E) The mass shift in the Asn form of an HSA reporter peptide after adding Amine-^{15}N $_L$-Gln, Amide-^{15}N $_L$-Gln and isotopically normal $_L$-Gln. (F) Validation of PSIAL activity in GOT1 protein with BLMH as a negative control. *$P < 0.05$, **$P < 0.01$, ***$P < 0.001$.

In summary, our findings in **Paper IV** suggested the existence of true repair of Asn deamidation, which can provide new insights for preventing aging and NDDs, as well as prolonging healthy lives.

5 CONCLUSIONS

Based on our findings above, we can conclude the following points.

Paper I – We obtained and characterized a mAb sensitive to isoAsp in HSA, the first of its kind, and based on that mAb developed an indirect ELISA demonstrating good specificity and sensitivity in quantification of the isoAsp level in human blood, which can be used for studying the link between isoAsp and AD. We also established the distribution of isoAsp levels in HSA of healthy blood for the first time.

Paper II – We proved for the first time that isoAsp-rich HSA forms aggregates with diminished binding ability toward Aß peptide and p-Tau protein. Through the ELISA developed in **Paper I**, we found increased isoAsp levels in HSA of AD blood, together with reduced levels of endogenous antibodies against aHSA, indicating hampered Aß and p-Tau clearance in AD. A new scenario of AD etiology is proposed.

Paper III – We demonstrated the capacity of isoAsp-related biomarkers in diagnosing NDDs at an early stage. The biomarker levels significantly correlated with cognitive decline, supporting the isoAsp role in NDD development. These biomarkers differentiated AD from PD, but were less specific in AD compared with other tested dementia types.

Paper IV – We explored the possibility of a full repair mechanism of isoAsp through theoretical considerations and presented the first experimental evidence of the existence of PSIAL activity, which repairs the ammonia loss from Asn.

6 POINTS OF PERSPECTIVE

According to the performance so far, the blood-based isoAsp biomarkers have shown very promising prospects in early diagnostics of NDDs. Additionally, isoAsp opens up new avenues for therapies to fight aging and NDDs. More specifically:

- **Clinically diagnostic** perspective: it is worth to further investigate the potential of isoAsp-related biomarkers in a broader longitudinal study to depict a more nuanced and complete picture of isoAsp role in early NDD diagnostics and disease progression. In particular, a larger cohort recruiting MCI participants should be included in a future study with follow-up data available to investigate the ability of isoAsp biomarkers to predict the cognitive decline and progression from MCI to probable AD or other NDDs. Besides, more types of NDD should be investigated, such as Huntington's disease (HD), amyotrophic lateral sclerosis (ALS), multiple sclerosis, etc., to fully define the specificity of isoAsp-related biomarkers in NDD diagnostics.
- **Fundamental** perspective: first, it will be interesting to determine the typical CDR sequences of antibodies in blood that specifically interact with aged HSA, thus revealing the disease-specific antibody sequences. Second, as the enzyme GOT1 with PSIAL activity could play a crucial role in the process of aging, further studies (both *in vitro* and *in vivo*) need to be carried out to specify its contribution to the relevant mechansim pathways.
- **Therapeutical** perspective: it is of high value to conduct isoAsp-related research in the treatment of NDDs based on the previous findings. On one hand, if the specific anti-aHSA antibodies could be extracted from healthy human blood, such antibodies can potentially be used in the therapy against NDDs, or in blood rejuvenation. The latter refers, e.g., to the clinical trial of transfusing blood plasma from young people to the patients with mild to medium AD, which warrants further studies to confirm the improvements of cognitive function and synaptic plasticity [165]. On the other hand, since SAM plays a very important role in isoAsp repair, both in the PIMT-mediated quick fix and in the PSIAL-mediated repair of isoAsp, it is probable that SAM deficiency participates in the NDD disease progression. Thus, dietary supplement of SAM in a regular and long term fashion starting from early disease stage may be beneficial for improving cognitive decline.

7 ACKNOWLEDGEMENTS

This has been a bumpy but fruitful journey, and I would not be where I am today without people who have supported me (not limited to those who are listed below) along the path.

First and foremost, I would like to express my sincere gratitude to my supervisor Prof. **Roman A. Zubarev**. Thank you for allowing me to join the lab and giving me such an appealing and challenging project. I still clearly remember the TED speech you shared with us on the first day I came to the lab, as you stressed that success depends highly on how determined a person is. Over the past years, I've gained a much deeper understanding of this sentence via each failure and success.

I am also grateful to my co-supervisor Dr. **Sergey Rodin**. Your guidance on carrying out biological research as well as career planning is really helpful for me. Thanks for motivating me to critically think about the project from more perspectives and maintain good habits throughout the research process. You are undoubtedly a nice role model for me as a professional scientist.

I would like to express my great appreciation to Prof. **Charlotte E. Teunissen** from Vrije Universiteit Amsterdam, Prof. **Jin-Tai Yu** from Fudan University and Dr. **Cong Guo** from Shanghai University, for the fantastic collaboration with you and your teams. Thank you for sharing not only the precious samples and techniques with us, but also your professional insights and advice. I've learnt a great deal through each discussion with you, and my dissertation would not have been shaped in such a broad way without your help. Thanks Prof. **Jin-Tai Yu** for accepting me as a visiting researcher in Huashan Hospital, Fudan University. I would also like to express my sincere thanks to the other co-authors: Dr. **Ya-Ru Zhang**, Dr. **Xue-Ning Shen**, Dr. **Maria D. Swan**, **Xin Chen**, Dr. **Jinming Han**, Prof. **Qiang Dong**, Prof. **Mei Cui**, and Prof. **Lan Tan**.

My appreciation also goes to my half-time review committee consisting of three AD experts, Prof. **Agneta Norberg**, Prof. **Charlotte E. Teunissen** and Dr. **Axel Abelein** for the constructive suggestions and valuable criticism for my project, which helped me proceed with my PhD study smoothly indeed.

Special thanks to Prof. **Henrik Zetterberg** for listening to my poster presentation and a pleasant discussion during the 2nd Swedish Meeting for Alzheimer Research. Thanks for expressing interest in my project and I am looking forward to collaboration in the future.

I am particularly thankful to **Susanna L. Lundström, Sven Seelow**, **Zhaowei Meng**, **Amir Ata Saei**, **Xuepei Zhang**, **Juan Astorga-Wells** and **Qinyu Jia**, for their important contribution to my PhD project. And I would like to appreciate **Akos Vegvari**, **Massimiliano Gaetani**, **Carina Palmberg** and **Marie Ståhlberg** for their always strong support of instrument maintenance, method optimization and troubleshooting. My thanks also go to the research students participating in my project, **Marcus Lundin, Arqum Anwar** and **Elif Değerli**, for their hard work and allowing me to gain teaching experience. Many thanks to all current and former members of Zubarev lab including but not limited to: **Hongqian Yang**, **Bo Zhang**, **Pierre Sabatier**, **Christian Beusch**, **Hassan Gharibi**, **Xueshu Xie**, **Pan Fang**, **Jin Wang**, **Alexey Chernobrovkin**, **Luciano Di Stefano**, **Giorgia Palano**, **Olga Lytovchenko**, **Jimmy**

Esneider Rodriguez, **Rahul Pandey**, **Yaroslav Lyuvinskiy**, **Piliang Hao**, **Zhenghe Lv**, **Yiqi Huang**, **Hongyu Xie**, **Yannan Gai**, **Weiqi Lu**, **Jimmy Ytterberg**, **Jaakko Teppo**, **Prajakta Naval**, **Sourav Mukherjee**, **Alexander Manoilov**, **Mohsen Ghasemi**, **Zhe Yang**, **Sze Wan Kennes Hung**, **Zhiwen Fu**, **Jilin He**, **Alexandra Alexandridou**, **Eleni Stergiou**, and **Muhammad Ikram**.

I also owe thanks to Prof. **Elias Arnér**, Prof. **Jesper Z. Haeggström** and their lab members for allowing me to use the instrument in their lab, as well as other support during the daily research life.

I am indebted to **Victoria Balabanova**, **Anneli Svarén** and **Alessandra Nanni** for helping me a lot with the administrative issues.

I extend my thanks to friends and colleagues in MBB who helped me every now and then: **Qing Cheng**, **Xiao Tang**, **Xiaoyuan Ren**, **Yang Wang**, **Taotao Li, Antonio Checa**, **Lucia Coppo**, and **Markus Dagnell**.

Cheers to my amazing friends in KI and Sweden: **Shuijie Li**, **Meng Yu**, **Huazhen Wang**, **Yanan Zong**, **Chenfei He**, **Chikai Zhou**, **Yuanyuan You**, **Yaxuan Liu**, **Le Tong**, **Ruining Liu**, **Hanxiong Li**, **Wen-Kuan Huang**, **Jingru Yu,** and **Hui Liu**. Thanks a lot for scientific discussion, fantastic foods, unforgettable trips and all the sweet memories we have in Sweden.

Special thanks go to Dr. **Xiaojun Xu** and Dr. **Jingxia Hao** for introducing me to Stockholm Lunar New Year Gala and many other cultural and arts events, which enriched my PhD life to a large extent. Thanks to all the friends I met in **斯京春晚**.

Thanks to the **China Scholarship Council (CSC)** who offered me the opportunity and support to accomplish my PhD study in Karolinska Institutet.

I also want to express my appreciation to all the **CSC scholars** and many other friends I encountered in Sweden. It is difficult to list all the names here, but I truly appreciate the support from all of you.

To my friends not in Sweden including but not limited to: **Lijie Ma**, **Yuwei Huang**, **Lu Xia**, **Jiawen Zhu**, **Sicen Chen**, and **Xin Su**. Thanks very much for always being there for me on the other side of the earth, which warmed me a lot especially during the dark winter seasons.

To my family, 感谢**爸爸**、**妈妈**的养育之恩，感恩你们为我塑造的开明宽松的成长环境以及一直以来最无私的支持和爱，让我有足够的勇气和力量在这个世界跌跌撞撞地自由探索。感谢**公公**、**婆婆**默默的支持和厚爱，愿你们身体健康，平安顺遂。

To my husband **Ziqing Chen**, it has been an exciting journey since we met before coming to Sweden, and only we could tell how amazing the stories have been. Thanks for all the funny, happy and difficult moments we've been through together. Let's see what the next chapter will be and cheers for our journey of being scientists.

8 REFERENCES

1. *World failing to address dementia challenge*. 2021; Available from: https://www.who.int/news/item/02-09-2021-world-failing-to-address-dementia-challenge.
2. Gaugler, J., et al., *2022 Alzheimer's disease facts and figures.* Alzheimers & Dementia, 2022. **18**(4): p. 700-789.
3. Price, J.L. and J.C. Morris, *Tangles and plaques in nondemented aging and "preclinical" Alzheimer's disease.* Ann Neurol, 1999. **45**(3): p. 358-68.
4. Mila-Aloma, M., M. Suarez-Calvet, and J.L. Molinuevo, *Latest advances in cerebrospinal fluid and blood biomarkers of Alzheimer's disease.* Ther Adv Neurol Disord, 2019. **12**: p. 1756286419888819.
5. Dubois, B., et al., *Clinical diagnosis of Alzheimer's disease: recommendations of the International Working Group.* Lancet Neurol, 2021. **20**(6): p. 484-496.
6. Louie, R., *The 2018 NIA-AA research framework: Recommendation and comments.* Alzheimers Dement, 2019. **15**(1): p. 182-183.
7. McKhann, G.M., et al., *The diagnosis of dementia due to Alzheimer's disease: Recommendations from the National Institute on Aging-Alzheimer's Association workgroups on diagnostic guidelines for Alzheimer's disease.* Alzheimer's & Dementia, 2011. **7**(3): p. 263-269.
8. Beach, T.G., et al., *Accuracy of the Clinical Diagnosis of Alzheimer Disease at National Institute on Aging Alzheimer Disease Centers, 2005-2010.* Journal of Neuropathology and Experimental Neurology, 2012. **71**(4): p. 266-273.
9. Rizzo, G., et al., *Accuracy of clinical diagnosis of dementia with Lewy bodies: a systematic review and meta-analysis.* J Neurol Neurosurg Psychiatry, 2018. **89**(4): p. 358-366.
10. Jellinger, K.A., et al., *Accuracy of clinical diagnosis of Parkinson disease: A systematic review and meta-analysis.* Neurology, 2016. **87**(2): p. 237-8.
11. Respondek, G., et al., *Validation of the movement disorder society criteria for the diagnosis of 4-repeat tauopathies.* Mov Disord, 2020. **35**(1): p. 171-176.
12. Hansson, O., *Biomarkers for neurodegenerative diseases.* Nat Med, 2021. **27**(6): p. 954-963.
13. Jack, C.R., et al., *NIA-AA Research Framework: Toward a biological definition of Alzheimer's disease.* Alzheimers & Dementia, 2018. **14**(4): p. 535-562.
14. Sheppard, O. and M. Coleman, *Alzheimer's Disease: Etiology, Neuropathology and Pathogenesis*, in *Alzheimer's Disease: Drug Discovery*, X. Huang, Editor. 2020: Brisbane (AU).
15. Fan, L., et al., *New Insights Into the Pathogenesis of Alzheimer's Disease.* Front Neurol, 2019. **10**: p. 1312.
16. Scheltens, P., et al., *Alzheimer's disease.* Lancet, 2021. **397**(10284): p. 1577-1590.

17. Hanon, O., et al., *Plasma amyloid levels within the Alzheimer's process and correlations with central biomarkers.* Alzheimers & Dementia, 2018. **14**(7): p. 858-868.

18. Park, J.C., et al., *Prognostic plasma protein panel for A beta deposition in the brain in Alzheimer's disease*. Progress in Neurobiology, 2019. **183**.

19. Paraskevaidi, M., et al., *Differential diagnosis of Alzheimer's disease using spectrochemical analysis of blood.* Proceedings of the National Academy of Sciences of the United States of America, 2017. **114**(38): p. E7929-E7938.

20. Mielke, M.M., et al., *Performance of plasma phosphorylated tau 181 and 217 in the community.* Nat Med, 2022. **28**(7): p. 1398-1405.

21. Ashton, N.J., et al., *Plasma p-tau231: a new biomarker for incipient Alzheimer's disease pathology.* Acta Neuropathol, 2021. **141**(5): p. 709-724.

22. Mattsson, N., et al., *Cerebrospinal fluid tau, neurogranin, and neurofilament light in Alzheimer's disease*. EMBO Mol Med, 2016. **8**(10): p. 1184-1196.

23. Blennow, K., *A Review of Fluid Biomarkers for Alzheimer's Disease: Moving from CSF to Blood.* Neurol Ther, 2017. **6**(Suppl 1): p. 15-24.

24. Bridel, C., et al., *Diagnostic Value of Cerebrospinal Fluid Neurofilament Light Protein in Neurology: A Systematic Review and Meta-analysis.* JAMA Neurol, 2019. **76**(9): p. 1035-1048.

25. Mattsson, N., et al., *Association Between Longitudinal Plasma Neurofilament Light and Neurodegeneration in Patients With Alzheimer Disease.* JAMA Neurol, 2019. **76**(7): p. 791-799.

26. Janelidze, S., et al., *Plasma beta-amyloid in Alzheimer's disease and vascular disease.* Sci Rep, 2016. **6**: p. 26801.

27. Palmqvist, S., et al., *Cerebrospinal fluid and plasma biomarker trajectories with increasing amyloid deposition in Alzheimer's disease.* EMBO Mol Med, 2019. **11**(12): p. e11170.

28. Milà-Alomà, M., et al., *Plasma p-tau231 and p-tau217 as state markers of amyloid-β pathology in preclinical Alzheimer's disease.* Nature Medicine, 2022.

29. Ray, S., et al., *Classification and prediction of clinical Alzheimer's diagnosis based on plasma signaling proteins.* Nat Med, 2007. **13**(11): p. 1359-62.

30. Mehta, P.D., et al., *A Sensitive and Cost-Effective Chemiluminescence ELISA for Measurement of Amyloid-beta 1-42 Peptide in Human Plasma.* Journal of Alzheimers Disease, 2020. **78**(3): p. 1237-1244.

31. Petzold, A., et al., *An ELISA for glial fibrillary acidic protein.* J Immunol Methods, 2004. **287**(1-2): p. 169-77.

32. Randall, J., et al., *Tau proteins in serum predict neurological outcome after hypoxic brain injury from cardiac arrest: results of a pilot study.* Resuscitation, 2013. **84**(3): p. 351-6.

33. Gisslen, M., et al., *Plasma Concentration of the Neurofilament Light Protein (NFL) is a Biomarker of CNS Injury in HIV Infection: A Cross-Sectional Study.* EBioMedicine, 2016. **3**: p. 135-140.

34. Rissin, D.M., et al., *Single-molecule enzyme-linked immunosorbent assay detects serum proteins at subfemtomolar concentrations.* Nat Biotechnol, 2010. **28**(6): p. 595-9.

35. Gaiottino, J., et al., *Increased Neurofilament Light Chain Blood Levels in Neurodegenerative Neurological Diseases.* Plos One, 2013. **8**(9).

36. Mielke, M.M., et al., *Plasma phospho-tau181 increases with Alzheimer's disease clinical severity and is associated with tau- and amyloid-positron emission tomography.* Alzheimers Dement, 2018. **14**(8): p. 989-997.

37. Zetterberg, H. and K. Blennow, *Moving fluid biomarkers for Alzheimer's disease from research tools to routine clinical diagnostics.* Mol Neurodegener, 2021. **16**(1): p. 10.

38. Abdelhak, A., et al., *Blood GFAP as an emerging biomarker in brain and spinal cord disorders.* Nat Rev Neurol, 2022. **18**(3): p. 158-172.

39. Hansson, O., et al., *The Alzheimer's Association appropriate use recommendations for blood biomarkers in Alzheimer's disease.* Alzheimers Dement, 2022.

40. Robinson, N.E. and A.B. Robinson, *Molecular clocks.* Proc Natl Acad Sci U S A, 2001. **98**(3): p. 944-9.

41. Peters, B. and B.L. Trout, *Asparagine deamidation: pH-dependent mechanism from density functional theory.* Biochemistry, 2006. **45**(16): p. 5384-92.

42. Johnson, B.A., et al., *Protein carboxyl methyltransferase facilitates conversion of atypical L-isoaspartyl peptides to normal L-aspartyl peptides.* J Biol Chem, 1987. **262**(12): p. 5622-9.

43. Flatmark, T. and K. Sletten, *Multiple forms of cytochrome c in the rat. Precursor-product relationship between the main component Cy I and the minor components Cy II and Cy 3 in vivo.* J Biol Chem, 1968. **243**(7): p. 1623-9.

44. Robinson, A.B., J.H. McKerrow, and M. Legaz, *Sequence dependent deamidation rates for model peptides of cytochrome C.* Int J Pept Protein Res, 1974. **6**(1): p. 31-5.

45. Robinson, A.B. and L.R. Robinson, *Distribution of Glutamine and Asparagine Residues and Their near Neighbors in Peptides and Proteins.* Proceedings of the National Academy of Sciences of the United States of America, 1991. **88**(20): p. 8880-8884.

46. Zhong, X. and J.F. Wright, *Biological insights into therapeutic protein modifications throughout trafficking and their biopharmaceutical applications.* International journal of cell biology, 2013. **2013**.

47. Doyle, H.A., R.J. Gee, and M.J. Mamula, *Altered immunogenicity of isoaspartate containing proteins.* Autoimmunity, 2007. **40**(2): p. 131-137.

48. Mamula, M.J., et al., *Isoaspartyl post-translational modification triggers autoimmune responses to self-proteins.* J Biol Chem, 1999. **274**(32): p. 22321-7.

49. Friedrich, M.G., et al., *Isoaspartic acid is present at specific sites in myelin basic protein from multiple sclerosis patients: could this represent a trigger for disease onset?* Acta neuropathologica communications, 2016. **4**(1): p. 83.

50. Wagner, A.M., et al., *Post-translational protein modifications in type 1 diabetes: a role for the repair enzyme protein-L-isoaspartate (D-aspartate) O-methyltransferase?* Diabetologia, 2007. **50**(3): p. 676-81.

51. Wagner, A.M., et al., *Posttranslational Protein Modifications in Type 1 Diabetes - Genetic Studies with PCMT1, the Repair Enzyme Protein Isoaspartate Methyltransferase (PIMT) Encoding Gene.* Rev Diabet Stud, 2008. **5**(4): p. 225-31.

52. Deverman, B.E., et al., *Bcl-X-L deamidation is a critical switch in the regulation of the response to DNA damage.* Cell, 2002. **111**(1): p. 51-62.

53. Lee, J.C., et al., *Protein L-isoaspartyl methyltransferase regulates p53 activity.* Nature Communications, 2012. **3**.

54. Goldberg, A.L., *Protein degradation and protection against misfolded or damaged proteins.* Nature, 2003. **426**(6968): p. 895-899.

55. Bohme, L., et al., *Isoaspartate residues dramatically influence substrate recognition and turnover by proteases.* Biological Chemistry, 2008. **389**(8): p. 1043-1053.

56. Cantor, J.R., et al., *The Human Asparaginase-like Protein 1 hASRGL1 Is an Ntn Hydrolase with beta-Aspartyl Peptidase Activity.* Biochemistry, 2009. **48**(46): p. 11026-11031.

57. Noronkoski, T., et al., *Glycosylasparaginase-catalyzed synthesis and hydrolysis of beta-aspartyl peptides.* Journal of Biological Chemistry, 1998. **273**(41): p. 26295-26297.

58. Schalk, A.M. and A. Lavie, *Structural and Kinetic Characterization of Guinea Pig L-Asparaginase Type III.* Biochemistry, 2014. **53**(14): p. 2318-2328.

59. Yang, H., et al., *Brain Proteomics Supports the Role of Glutamate Metabolism and Suggests Other Metabolic Alterations in Protein L-Isoaspartyl Methyltransferase (PIMT)-Knockout Mice.* Journal of Proteome Research, 2013. **12**(10): p. 4566-4576.

60. Kim, E., et al., *Deficiency of a protein-repair enzyme results in the accumulation of altered proteins, retardation of growth, and fatal seizures in mice.* Proceedings of the National Academy of Sciences of the United States of America, 1997. **94**(12): p. 6132-6137.

61. Yamamoto, A., et al., *Deficiency in protein L-isoaspartyl methyltransferase results in a fatal progressive epilepsy.* Journal of Neuroscience, 1998. **18**(6): p. 2063-2074.

62. Farrar, C., C.R. Houser, and S. Clarke, *Activation of the PI3K/Akt signal transduction pathway and increased levels of insulin receptor in protein repair-deficient mice.* Aging Cell, 2005. **4**(1): p. 1-12.

63. MacKay, K.B., J.D. Lowenson, and S.G. Clarke, *Wortmannin Reduces Insulin Signaling and Death in Seizure-Prone Pcmt1(-/-) Mice.* Plos One, 2012. **7**(10).

64. Kosugi, S., et al., *Suppression of protein l-isoaspartyl (d-aspartyl) methyltransferase results in hyperactivation of EGF-stimulated MEK-ERK signaling in cultured mammalian cells.* Biochem Biophys Res Commun, 2008. **371**(1): p. 22-7.

65. Levitt, D.G. and M.D. Levitt, *Human serum albumin homeostasis: a new look at the roles of synthesis, catabolism, renal and gastrointestinal excretion, and the clinical value of serum albumin measurements.* International Journal of General Medicine, 2016. **9**: p. 229-255.

66. Hao, X., et al., *Immunoassay of S-adenosylmethionine and S-adenosylhomocysteine: the methylation index as a biomarker for disease and health status.* BMC Res Notes, 2016. **9**(1): p. 498.

67. Perna, A.F., et al., *Plasma proteins containing damaged L-isoaspartyl residues are increased in uremia: Implications for mechanism.* Kidney International, 2001. **59**(6): p. 2299-2308.

68. Yang, H. and R.A. Zubarev, *Mass spectrometric analysis of asparagine deamidation and aspartate isomerization in polypeptides.* Electrophoresis, 2010. **31**(11): p. 1764-72.

69. Johnson, B.A. and D.W. Aswad, *Optimal Conditions for the Use of Protein L-Isoaspartyl Methyltransferase in Assessing the Isoaspartate Content of Peptides and Proteins.* Analytical Biochemistry, 1991. **192**(2): p. 384-391.

70. Shimizu, T., et al., *Isoaspartate formation and neurodegeneration in Alzheimer's disease.* Archives of Biochemistry and Biophysics, 2000. **381**(2): p. 225-234.

71. Yamamoto, A., et al., *Deficiency in protein L-isoaspartyl methyltransferase results in a fatal progressive epilepsy.* J Neurosci, 1998. **18**(6): p. 2063-74.

72. Johnson, B.A., et al., *Protein L-Isoaspartyl Methyltransferase in Postmortem Brains of Aged Humans.* Neurobiology of Aging, 1991. **12**(1): p. 19-24.

73. Moro, M.L., et al., *Pyroglutamate and Isoaspartate modified Amyloid-Beta in ageing and Alzheimer's disease.* Acta Neuropathologica Communications, 2018. **6**.

74. Tjernberg, L.O., et al., *A molecular model of Alzheimer amyloid beta-peptide fibril formation.* J Biol Chem, 1999. **274**(18): p. 12619-25.

75. Chatterjee, T., et al., *The role of isoaspartate in fibrillation and its prevention by Protein-L-isoaspartyl methyltransferase.* Biochim Biophys Acta Gen Subj, 2020. **1864**(3): p. 129500.

76. Roher, A.E., et al., *Structural Alterations in the Peptide Backbone of Beta-Amyloid Core Protein May Account for Its Deposition and Stability in Alzheimers-Disease.* Journal of Biological Chemistry, 1993. **268**(5): p. 3072-3083.

77. Fukuda, H., et al., *Synthesis, aggregation, and neurotoxicity of the Alzheimer's A beta 1-42 amyloid peptide and its isoaspartyl isomers.* Bioorganic & Medicinal Chemistry Letters, 1999. **9**(7): p. 953-956.

78. Sugiki, T. and N. Utsunomiya-Tate, *Site-specific aspartic acid isomerization regulates self-assembly and neurotoxicity of amyloid-beta.* Biochemical and Biophysical Research Communications, 2013. **441**(2): p. 493-498.

79. Kozin, S.A., et al., *Peripherally Applied Synthetic Peptide isoAsp7-A beta(1-42) Triggers Cerebral beta-Amyloidosis.* Neurotoxicity Research, 2013. **24**(3): p. 370-376.

80. Shimizu, T., Y. Matsuoka, and T. Shirasawa, *Biological significance of isoaspartate and its repair system.* Biol Pharm Bull, 2005. **28**(9): p. 1590-6.

81. de Leon, M.J. and K. Blennow, *Therapeutic potential for peripheral clearance of misfolded brain proteins.* Nature Reviews Neurology, 2018. **14**(11): p. 637-638.

82. Maarouf, C.L., et al., *Impaired hepatic amyloid-beta degradation in Alzheimer's disease.* Plos One, 2018. **13**(9).

83. Sehgal, N., et al., *Withania somnifera reverses Alzheimer's disease pathology by enhancing low-density lipoprotein receptor-related protein in liver.* Proc Natl Acad Sci U S A, 2012. **109**(9): p. 3510-5.

84. Liu, Y.H., et al., *Clearance of Amyloid-Beta in Alzheimer's Disease: Shifting the Action Site from Center to Periphery.* Molecular Neurobiology, 2015. **51**(1): p. 1-7.

85. Yang, H., et al., *Alzheimer's disease and mild cognitive impairment are associated with elevated levels of isoaspartyl residues in blood plasma proteins.* J Alzheimers Dis, 2011. **27**(1): p. 113-8.

86. Yang, H.Q., et al., *Prognostic Polypeptide Blood Plasma Biomarkers of Alzheimer's Disease Progression.* Journal of Alzheimers Disease, 2014. **40**(3): p. 659-666.

87. Cortes-Canteli, M., et al., *Fibrinogen and altered hemostasis in Alzheimer's disease.* J Alzheimers Dis, 2012. **32**(3): p. 599-608.

88. Carter, D.C. and J.X. Ho, *Structure of Serum-Albumin.* Advances in Protein Chemistry, Vol 45, 1994. **45**: p. 153-203.

89. Doweiko, J.P. and D.J. Nompleggi, *Role of Albumin in Human Physiology and Pathophysiology.* Journal of Parenteral and Enteral Nutrition, 1991. **15**(2): p. 207-211.

90. Tessari, P., *Protein metabolism in liver cirrhosis: from albumin to muscle myofibrils.* Current Opinion in Clinical Nutrition and Metabolic Care, 2003. **6**(1): p. 79-85.

91. Bal, W., et al., *Binding of transition metal ions to albumin: Sites, affinities and rates.* Biochimica Et Biophysica Acta-General Subjects, 2013. **1830**(12): p. 5444-5455.

92. Bhattacharya, A.A., T. Grune, and S. Curry, *Crystallographic analysis reveals common modes of binding of medium and long-chain fatty acids to human serum albumin.* Journal of Molecular Biology, 2000. **303**(5): p. 721-732.

93. Zunszain, P.A., et al., *Crystal structural analysis of human serum albumin complexed with hemin and fatty acid.* BMC Struct Biol, 2003. **3**: p. 6.

94. Petitpas, I., et al., *Structural basis of albumin-thyroxine interactions and familial dysalbuminemic hyperthyroxinemia.* Proceedings of the National Academy of Sciences of the United States of America, 2003. **100**(11): p. 6440-6445.

95. Bertucci, C. and E. Domenici, *Reversible and covalent binding of drugs to human serum albumin: Methodological approaches and physiological relevance.* Current Medicinal Chemistry, 2002. **9**(15): p. 1463-1481.

96. Biere, A.L., et al., *Amyloid beta-peptide is transported on lipoproteins and albumin in human plasma.* Journal of Biological Chemistry, 1996. **271**(51): p. 32916-32922.

97. Milojevic, J. and G. Melacini, *Stoichiometry and Affinity of the Human Serum Albumin-Alzheimer's A beta Peptide Interactions.* Biophysical Journal, 2011. **100**(1): p. 183-192.

98. Picon-Pages, P., et al., *Human Albumin Impairs Amyloid beta-peptide Fibrillation Through its C-terminus: From docking Modeling to Protection Against Neurotoxicity in Alzheimer's disease.* Computational and Structural Biotechnology Journal, 2019. **17**: p. 963-971.

99. Stanyon, H.F. and J.H. Viles, *Human serum albumin can regulate amyloid-beta peptide fiber growth in the brain interstitium: Implications for Alzheimer disease.* Journal of Biological Chemistry, 2012. **287**(33): p. 28163-28168.

100. Milojevic, J., A. Raditsis, and G. Melacini, *Human Serum Albumin Inhibits A beta Fibrillization through a "Monomer-Competitor" Mechanism.* Biophysical Journal, 2009. **97**(9): p. 2585-2594.

101. Inoue, M., et al., *Serum Levels of Albumin-beta-Amyloid Complex in Patients with Depression.* Am J Geriatr Psychiatry, 2016. **24**(9): p. 764-72.

102. Mizrahi, E.H., et al., *Serum albumin levels predict cognitive impairment in elderly hip fracture patients.* American Journal of Alzheimers Disease and Other Dementias, 2008. **23**(1): p. 85-90.

103. Llewellyn, D.J., et al., *Serum Albumin Concentration and Cognitive Impairment.* Current Alzheimer Research, 2010. **7**(1): p. 91-96.

104. Maes, M., et al., *Inflammatory markers in younger vs elderly normal volunteers and in patients with Alzheimer's disease.* Journal of Psychiatric Research, 1999. **33**(5): p. 397-405.

105. Kim, T.S., et al., *Decreased plasma antioxidants in patients with Alzheimer's disease.* International Journal of Geriatric Psychiatry, 2006. **21**(4): p. 344-348.

106. Chio, A., et al., *Amyotrophic Lateral Sclerosis Outcome Measures and the Role of Albumin and Creatinine A Population-Based Study.* Jama Neurology, 2014. **71**(9): p. 1134-1142.

107. LeVine, S.M., *Albumin and multiple sclerosis.* BMC Neurol, 2016. **16**: p. 47.

108. Sun, J., et al., *Blood biomarkers and prognosis of amyotrophic lateral sclerosis.* European Journal of Neurology, 2020. **27**(11): p. 2125-2133.

109. Kim, J.W., et al., *Serum albumin and beta-amyloid deposition in the human brain.* Neurology, 2020. **95**(7): p. E815-E826.

110. Morrison, L.D., D.D. Smith, and S.J. Kish, *Brain S-adenosylmethionine levels are severely decreased in Alzheimer's disease.* J Neurochem, 1996. **67**(3): p. 1328-31.

111. Bottiglieri, T., et al., *Cerebrospinal fluid S-adenosylmethionine in depression and dementia: effects of treatment with parenteral and oral S-adenosylmethionine.* J Neurol Neurosurg Psychiatry, 1990. **53**(12): p. 1096-8.

112. Linnebank, M., et al., *S-adenosylmethionine is decreased in the cerebrospinal fluid of patients with Alzheimer's disease.* Neurodegener Dis, 2010. **7**(6): p. 373-8.

113. Bal, W., et al., *Multi-metal binding site of serum albumin.* Journal of Inorganic Biochemistry, 1998. **70**(1): p. 33-39.

114. Lovell, M.A., et al., *Copper, iron and zinc in Alzheimer's disease senile plaques.* Journal of the Neurological Sciences, 1998. **158**(1): p. 47-52.

115. Bush, A.I. and R.E. Tanzi, *Therapeutics for Alzheimer's disease based on the metal hypothesis.* Neurotherapeutics, 2008. **5**(3): p. 421-32.

116. Perrone, L., et al., *Copper Transfer from Cu-A beta to Human Serum Albumin Inhibits Aggregation, Radical Production and Reduces A beta Toxicity.* Chembiochem, 2010. **11**(1): p. 110-118.

117. Zubcic, K., et al., *The Role of Copper in Tau-Related Pathology in Alzheimer's Disease.* Front Mol Neurosci, 2020. **13**: p. 572308.

118. Reiber, H. and J.B. Peter, *Cerebrospinal fluid analysis: disease-related data patterns and evaluation programs.* J Neurol Sci, 2001. **184**(2): p. 101-22.

119. Skillback, T., et al., *CSF/serum albumin ratio in dementias: a cross-sectional study on 1861 patients.* Neurobiol Aging, 2017. **59**: p. 1-9.

120. Piro, A., et al., *Paul Ehrlich: the Nobel Prize in physiology or medicine 1908.* Int Rev Immunol, 2008. **27**(1-2): p. 1-17.

121. Kohler, G. and C. Milstein, *Continuous Cultures of Fused Cells Secreting Antibody of Predefined Specificity.* Nature, 1975. **256**(5517): p. 495-497.

122. Karsten, U., et al., *Direct Comparison of Electric Field-Mediated and Peg-Mediated Cell-Fusion for the Generation of Antibody-Producing Hybridomas.* Hybridoma, 1988. **7**(6): p. 627-633.

123. Committee on Methods of Producing Monoclonal Antibodies, I.f.L.A.R., National Research Council, *Monoclonal antibody production*. Vol. 7. 1999: National Academy Press. 57.

124. Lipman, N.S., et al., *Monoclonal versus polyclonal antibodies: Distinguishing characteristics, applications, and information resources.* Ilar Journal, 2005. **46**(3): p. 258-268.

125. Kaplon, H. and J.M. Reichert, *Antibodies to watch in 2019.* Mabs, 2019. **11**(2): p. 219-238.

126. Kaplon, H., et al., *Antibodies to watch in 2020.* Mabs, 2020. **12**(1).

127. Kaplon, H. and J.M. Reichert, *Antibodies to watch in 2021.* Mabs, 2021. **13**(1).

128. Reichert, J.M. *Antibody therapeutics approved or in regulatory review in the EU or US.* May 1, 2021 May 1, 2021]; Available from: https://www.antibodysociety.org/resources/approved-antibodies/.

129. Lu, R.M., et al., *Development of therapeutic antibodies for the treatment of diseases.* Journal of Biomedical Science, 2020. **27**(1).

130. Kelley, B., *Developing therapeutic monoclonal antibodies at pandemic pace.* Nature Biotechnology, 2020. **38**(5): p. 540-545.

131. Larrick, J.W., et al., *Rapid Cloning of Rearranged Immunoglobulin Genes from Human Hybridoma Cells Using Mixed Primers and the Polymerase Chain-Reaction.* Biochemical and Biophysical Research Communications, 1989. **160**(3): p. 1250-1256.

132. Boyd, S.D. and J.E. Crowe, *Deep sequencing and human antibody repertoire analysis.* Current Opinion in Immunology, 2016. **40**: p. 103-109.

133. Barderas, R. and E. Benito-Pena, *The 2018 Nobel Prize in Chemistry: phage display of peptides and antibodies.* Analytical and Bioanalytical Chemistry, 2019. **411**(12).

134. Ravn, U., et al., *Deep sequencing of phage display libraries to support antibody discovery.* Methods, 2013. **60**(1): p. 99-110.

135. Yang, W., et al., *Next-generation sequencing enables the discovery of more diverse positive clones from a phage-displayed antibody library.* Exp Mol Med, 2017. **49**(3): p. e308.

136. Georgiou, G., et al., *The promise and challenge of high-throughput sequencing of the antibody repertoire.* Nature Biotechnology, 2014. **32**(2): p. 158-168.

137. Cheung, W.C., et al., *A proteomics approach for the identification and cloning of monoclonal antibodies from serum.* Nature Biotechnology, 2012. **30**(5): p. 447-+.

138. Guthals, A., et al., *De Novo MS/MS Sequencing of Native Human Antibodies.* Journal of Proteome Research, 2017. **16**(1): p. 45-54.

139. Tran, N.H., et al., *Complete De Novo Assembly of Monoclonal Antibody Sequences.* Scientific Reports, 2016. **6**.

140. Wright, A. and S.L. Morrison, *Effect of glycosylation on antibody function: Implications for genetic engineering.* Trends in Biotechnology, 1997. **15**(1): p. 26-32.

141. Jennewein, M.F. and G. Alter, *The Immunoregulatory Roles of Antibody Glycosylation.* Trends in Immunology, 2017. **38**(5): p. 358-372.

142. Kaur, H., *Characterization of glycosylation in monoclonal antibodies and its importance in therapeutic antibody development.* Critical Reviews in Biotechnology, 2021. **41**(2): p. 300-315.

143. Fonseca, M.I., et al., *The presence of isoaspartic acid in beta-amyloid plaques indicates plaque age.* Experimental Neurology, 1999. **157**(2): p. 277-288.

144. Laird, I.A., et al., *Methods and compositions for detecting, imaging, and treating small cell lung cancer utilizing post-translationally modified residues and higher molecular weight antigenic complexes in proteins*. 2014, Google Patents.

145. Gnoth, K., et al., *Targeting isoaspartate-modified Abeta rescues behavioral deficits in transgenic mice with Alzheimer's disease-like pathology.* Alzheimers Res Ther, 2020. **12**(1): p. 149.

146. Jack, C.R., Jr., et al., *NIA-AA Research Framework: Toward a biological definition of Alzheimer's disease.* Alzheimers Dement, 2018. **14**(4): p. 535-562.

147. Willemse, E.A.J., et al., *Diagnostic performance of Elecsys immunoassays for cerebrospinal fluid Alzheimer's disease biomarkers in a nonacademic, multicenter memory clinic cohort: The ABIDE project.* Alzheimers Dement (Amst), 2018. **10**: p. 563-572.

148. Xu, W., et al., *Amyloid Pathologies Modulate the Associations of Minimal Depressive Symptoms With Cognitive Impairments in Older Adults Without Dementia.* Biol Psychiatry, 2021. **89**(8): p. 766-775.

149. Hu, H., et al., *Tau pathologies mediate the association of blood pressure with cognitive impairment in adults without dementia: The CABLE study.* Alzheimers Dement, 2021.

150. Xu, W., et al., *Sleep characteristics and cerebrospinal fluid biomarkers of Alzheimer's disease pathology in cognitively intact older adults: The CABLE study.* Alzheimers Dement, 2020. **16**(8): p. 1146-1152.

151. McKhann, G., et al., *Clinical diagnosis of Alzheimer's disease: report of the NINCDS-ADRDA Work Group under the auspices of Department of Health and Human Services Task Force on Alzheimer's Disease.* Neurology, 1984. **34**(7): p. 939-44.

152. Jack, C.R., Jr., et al., *Introduction to the recommendations from the National Institute on Aging-Alzheimer's Association workgroups on diagnostic guidelines for Alzheimer's disease.* Alzheimers Dement, 2011. **7**(3): p. 257-62.

153. Roman, G.C., et al., *Vascular dementia: diagnostic criteria for research studies. Report of the NINDS-AIREN International Workshop.* Neurology, 1993. **43**(2): p. 250-60.

154. Rascovsky, K., et al., *Sensitivity of revised diagnostic criteria for the behavioural variant of frontotemporal dementia.* Brain, 2011. **134**(Pt 9): p. 2456-77.

155. Postuma, R.B., et al., *MDS clinical diagnostic criteria for Parkinson's disease.* Mov Disord, 2015. **30**(12): p. 1591-601.

156. Noguchi, S., K. Miyawaki, and Y. Satow, *Succinimide and isoaspartate residues in the crystal structures of hen egg-white lysozyme complexed with tri-N-acetylchitotriose.* J Mol Biol, 1998. **278**(1): p. 231-8.

157. Mateus, A., T.A. Maatta, and M.M. Savitski, *Thermal proteome profiling: unbiased assessment of protein state through heat-induced stability changes.* Proteome Sci, 2016. **15**: p. 13.

158. Zhang, Y.R., et al., *Peripheral immunity is associated with the risk of incident dementia.* Molecular Psychiatry, 2022.

159. Richartz, E., et al., *Decline of immune responsiveness: A pathogenetic factor in Alzheimer's disease?* Journal of Psychiatric Research, 2005. **39**(5): p. 535-543.

160. Park, J.E., et al., *Aging-induced isoDGR-modified fibronectin activates monocytic and endothelial cells to promote atherosclerosis.* Atherosclerosis, 2021. **324**: p. 58-68.

161. Russell, J.B. and H.J. Strobel, *Concentration of ammonia across cell membranes of mixed rumen bacteria.* J Dairy Sci, 1987. **70**(5): p. 970-6.

162. Konuklar, F.A., et al., *Modeling the deamidation of asparagine residues via succinimide intermediates.* Molecular modeling annual, 2001. **7**(5): p. 147-160.

163. Catak, S., et al., *Deamidation of asparagine residues: direct hydrolysis versus succinimide-mediated deamidation mechanisms.* J Phys Chem A, 2009. **113**(6): p. 1111-20.

164. Peracchi, A., *The Limits of Enzyme Specificity and the Evolution of Metabolism.* Trends Biochem Sci, 2018. **43**(12): p. 984-996.

165. Sha, S.J., et al., *Safety, Tolerability, and Feasibility of Young Plasma Infusion in the Plasma for Alzheimer Symptom Amelioration Study: A Randomized Clinical Trial.* JAMA Neurol, 2019. **76**(1): p. 35-40.